NAVAL POSTGRADUATE SCHOOL
Monterey, California

THESIS

PERFORMANCE ANALYSIS OF ADAPTIVE ANTENNA WITH CODING AND RAKE RECEIVER

by

Kaiser Tan Beng Kiat

March 2002

Thesis Advisor:	Tri T. Ha
Second Reader:	David Jenn

REPORT DOCUMENTATION PAGE			Form Approved OMB No. 0704-0188
Public reporting burden for this collection of information is estimated to average 1 hour per response, including the time for reviewing instruction, searching existing data sources, gathering and maintaining the data needed, and completing and reviewing the collection of information. Send comments regarding this burden estimate or any other aspect of this collection of information, including suggestions for reducing this burden, to Washington headquarters Services, Directorate for Information Operations and Reports, 1215 Jefferson Davis Highway, Suite 1204, Arlington, VA 22202-4302, and to the Office of Management and Budget, Paperwork Reduction Project (0704-0188) Washington DC 20503.			
1. AGENCY USE ONLY *(Leave blank)*	**2. REPORT DATE** March 2002	**3. REPORT TYPE AND DATES COVERED** Master's Thesis	
4. TITLE AND SUBTITLE: Performance analysis of adaptive antenna with coding and rake receiver			**5. FUNDING NUMBERS**
6. AUTHOR Kaiser Tan Beng Kiat			
7. PERFORMING ORGANIZATION NAME AND ADDRESS Naval Postgraduate School Monterey, CA 93943-5000			**8. PERFORMING ORGANIZATION REPORT NUMBER**
9. SPONSORING / MONITORING AGENCY NAME(S) AND ADDRESS(ES) N/A			**10. SPONSORING / MONITORING AGENCY REPORT NUMBER**
11. SUPPLEMENTARY NOTES The views expressed in this thesis are those of the author and do not reflect the official policy or position of the Department of Defense or the U.S. Government.			
12a. DISTRIBUTION / AVAILABILITY STATEMENT Approved for public release; distribution is unlimited.			**12b. DISTRIBUTION CODE**

In this thesis, we presented the analytical expressions for probability of bit error (BER), the probability density function (PDF) and cumulative distribution function (CDF) of the output signal-to-noise-plus-interference ratio (SINR) of an adaptive antenna operating in multipath environments with multiple interferers and flat Rayleigh fading. The analytical expressions for BER, PDF and CDF were then developed including the effect of coding and the use of RAKE receiver. The performance of adaptive antenna with and without coding as well as with RAKE receiver was analyzed and compared.

14. SUBJECT TERMS Wireless, Performance Analysis, Rayleigh, RAKE Receiver, Convolutional Codes, Adaptive Antenna Arrays.			**15. NUMBER OF PAGES** 72
			16. PRICE CODE
17. SECURITY CLASSIFICATION OF REPORT Unclassified	**18. SECURITY CLASSIFICATION OF THIS PAGE** Unclassified	**19. SECURITY CLASSIFICATION OF ABSTRACT** Unclassified	**20. LIMITATION OF ABSTRACT** UL

NSN 7540-01-280-5500 Standard Form 298 (Rev. 2-89)
Prescribed by ANSI Std. 239-18

THIS PAGE INTENTIONALLY LEFT BLANK

Approved for public release; distribution is unlimited.

PERFORMANCE ANALYSIS OF ADAPTIVE ANTENNA WITH CODING AND RAKE RECEIVER

Kaiser Tan Beng Kiat
Major, Singapore Army
B.E., Nanyang Technological University, 1993

Submitted in partial fulfillment of the
requirements for the degree of

MASTER OF SCIENCE IN ELECTRICAL ENGINEERING

from the

NAVAL POSTGRADUATE SCHOOL
March 2002

Author: Kaiser Tan Beng Kiat

Approved by: Tri T. Ha, Thesis Advisor

Jovan Lebaric, Co-Advisor

David Jenn, Second Reader

Jeffrey B. Knorr, Chairman
Department of Electrical and Computer Engineering

THIS PAGE INTENTIONALLY LEFT BLANK

ABSTRACT

In this thesis, we presented the analytical expressions for probability of bit error (BER), the probability density function (PDF) and cumulative distribution function (CDF) of the output signal-to-noise-plus-interference ratio (SINR) of an adaptive antenna operating in multipath environments with multiple interferers and flat Rayleigh fading. The analytical expressions for BER, PDF and CDF were then developed including the effect of coding and the use of RAKE receiver. The performance of adaptive antenna with and without coding as well as with RAKE receiver was analyzed and compared. The expression derived, in terms of the mean eigenvalues of the system, is accurate based on an approximation to the characteristic function of the output signal-to-interference-plus-noise ratio (SINR). As a result, a closed form expression of bit error rate (BER) for coherent phase-shift keying (PSK) has been derived for adaptive antenna array working with coding and RAKE receiver.

THIS PAGE INTENTIONALLY LEFT BLANK

TABLE OF CONTENTS

THIS PAGE INTENTIONALLY LEFT BLANK

LIST OF FIGURES

LIST OF TABLES

THIS PAGE INTENTIONALLY LEFT BLANK

ACKNOWLEDGMENTS

I wish to express my sincerest appreciation to my advisors, Professor Tri. Ha Without his support, clear explanations and supervision this thesis would not have been possible.

I want to thank Professor Lebaric for his contributions.

I also wish to thank my family, my loving wife, Kit Yi and my beautiful daughter, Raeann, for their understanding, support and love.

Last but not least, I would like to thank God for his kindness and love that sustain me throughout the entire course.

THIS PAGE INTENTIONALLY LEFT BLANK

EXECUTIVE SUMMARY

The presence of cochannel interference in the cellular system has limited the system capacity. In order to meet the ever-growing demand of high data rates with the limited spectrum available, system designers are exploring new ideas to increase the system capacity and meet all the demand.

This thesis addresses the performance of adaptive antenna array that will increase the system capacity by rejecting the interference and improving the output signal-to-interference-plus-noise (SINR). The analytical expressions for the cumulative distribution function (CDF), the probability density function (PDF) and the Bit Error Rate (BER) for the adaptive antenna array working with channel coding over a flat Rayleigh fading channel are developed. These expressions are givenin terms of eigenvalues of the system based on an approximation to the characteristic function of the output SINR. We assume that the antenna branches are uncorrelated and equal power gain at all the antenna branches. A block diagram of an adaptive antenna array system is illustrated in Figure 1.

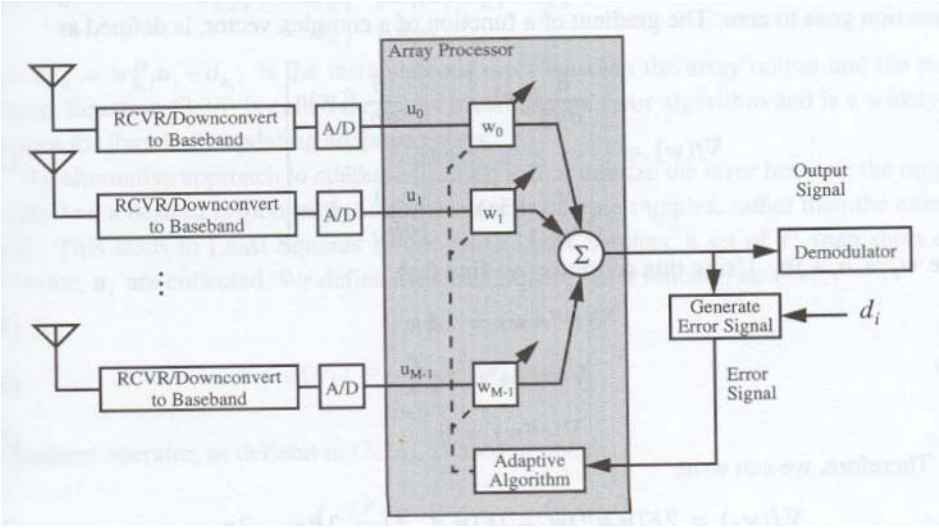

Figure 1. Block diagram of an adaptive antenna system.

The results show that these expressions are accurate even though they are based on an approximation. The analytical results also show that by using forward error correction (FEC), the system performance can be greatly enhanced due to the substantial coding gain. Furthermore, in a multipath environment, the user's signal has distinct fading statistics due to different propagation paths over which it travels. A RAKE receiver can be used to combine the useful information obtained from the resolvable multipath components and improve the overall signal-to-noise ratio. Similarly, using the same approach, the analytical expressions for the PDF, and BER for an adaptive antenna with RAKE receiver and with coding are also derived. Figure 2 shows the typical RAKE receiver model.

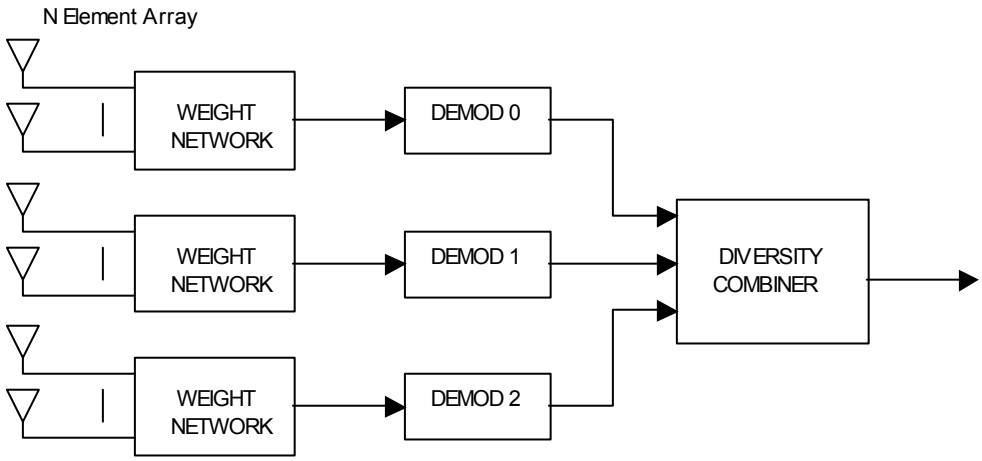

Figure 2. Typical RAKE receiver model.

The results show that by using FEC with an adaptive antenna array, the BER performance can be greatly improved.

I. INTRODUCTION

In wireless communications, the presence of cochannel interference limits the system capacity, whereas multipath fading limits the system performance. In addition, with the limited spectrum and ever increasing demand to accommodate more users and new high data rate services such as video conferencing and multi-media wideband services in the third generation mobile communication systems (3G), cellular and wireless operators are exploring new ideas to increase the system capacity and meet all the demand.

Smart antennas, or adaptive antenna arrays in particular, have been shown to combat both multipath fading of the desired signal and cochannel interference, increasing the performance of mobile radio communication systems. Optimum combining using an adaptive antenna array was studied for both faded [1] and non-faded [2] communications. With optimum combining, the signals received by several antenna elements are weighted and combined to maximize the output signal-to-interference-plus-noise ratio (SINR).

In the absence of interference, and with noise as the only undesired signal, an adaptive antenna performs the same task as a diversity antenna with maximal ratio combining (MRC). The performance of adaptive antennas with multiple interferers and flat Rayleigh fading has been studied by many researchers, such as T.D. Pham and K.G. Balmain [3], R. Janaswamy [4], and C. Liberti [10]. In this thesis, we study the performance of adaptive antenna with coding as well as RAKE receiver. We also develop an analytical expression for the PDF and theCDF of the output SINR, and derive the BER expression for adaptive antennas with coding and RAKE receiver.

By using convolutional coding with Viterbi soft decision decoding, the system performance can be greatly enhanced due to the substantial coding gain. Channel coding improves mobile communication link performance by adding redundant data bits in the transmitted data so that the receiver can detect or correct some (or all) of the errors introduced by the channel. RAKE receiver combines the useful information obtained from several resolvable multipath components and improves the signal to noise ratio.

Chapter II presents an overview of smart antenna technology that can improve the system performance. Chapter III presents the computation of optimal weights for a narrowband signal, output SINR, statistics of the output SINR in terms of the PDF and the CDF , as well as the BER performance of an adaptive antenna without coding which was studied by T.D. Pham and K.G. Balmain [3] and R. Janaswamy [4]. In Chapter IV, we develop the analytical expression for the PDF, CDF, output SINR and the BER for adaptive antennas with coding effect. Chapter V presents the effect of RAKE receiver. The BER performance was analyzed and compared between adaptive antennas with and without coding in Chapter VI. In Chapter VII, we present a summary and the conclusions.

II. OVERVIEW OF SMART ANTENNA TECHNOLOGY

The radio frequency spectrum is a finite and valuable resource. For a fixed bandwidth of spectrum, there is a fundamental limit on the number of radio channels that can be realized by a mobile communication system operating over this bandwidth. Anticipating these limits, considerable amount of work has been done on the use of time, frequency and coding techniques to increase the capacity and some of this effort has resulted in multiple-access standards, such as frequency-division multiple access (FDMA), time-division multiple access (TDMA), and code-division multiple access (CDMA). Recently, there has been tremendous increase in subscribers for cellular and personal communication systems and this trend is expected to continue in the years to come. Furthermore, growth in data services is pushing these systems beyond their capacities. To meet the demand for subscriber growth, wireless operators need practical, cost-effective infrastructure solutions that enhance network capacity and coverage. This is a major consideration for second generation (2G) mobile/cellular operators as they plan for growth. In addition, the proposed third generation (3G) mobile communication networks will also be prone to the problem of spectral congestion as the number of subscribers increases and services are expanded [5].

Antenna arrays when used in an appropriate configuration, at the base station, in mobile communications offer significant benefits in system performance by increasing channel capacity and spectrum efficiency. Arrays can also help reduce multipath fading and increasecoverage. Such antenna arrays are known as smart antennas. Smart antennas are a solution to capacity and interference problems. Most smart antennas form beams directed to a particular user in order to enhance the received signal strength and signal-to-noise ratio (SNR).

Smart antennas are classified into two main types: Switched Beam and Digitally Adaptive Beamformers (DAB). A switched beam antenna system consists of several highly directive, fixed, pre-defined beams, formed usually with fixed antenna arrays. It measures RF power or signal strength from a set of pre-defined beams and outputs RF from the selected beams that give the best performance to a desired user. In a DAB antenna system, adaptive techniques are used to enhance the radio link. The signals are

first down-converted to an intermediate frequency (IF), then digitized, weighted and summed in a pre-defined processing algorithm. In general, all smart antennas direct their main beam with increased gain, in the direction of the user (they may direct nulls in the direction of the interfering signal as well). Although both switched beam and DAB systems have this in common, only the DAB system offers optimal gain, while simultaneously identifying, tracking, and minimizing reception of interfering signals. The DAB system's null forming capability offers substantial performance advantages over the more passive switched beam approach by enabling the maximum interference suppression.

DAB systems are further classified into two types: dynamic phased arrays and adaptive antenna arrays. Dynamic phased arrays make use of the direction of arrival (DoA) information from the desired user and steer a beam maximum towards the desired user. This allows continuous tracking of the user, thus improving upon the capabilities of a switched beam antenna. In an adaptive antenna array, the weights are adjusted to maximize the signal-to-interference-plus-noise ratio (SINR) and provide the maximum discrimination against interfering signals. In the absence of interferers and with noise as the only undesired signal, adaptive antennas maximize the signal-to-noise ratio (SNR), and thus behave as a maximum ratio combiner (MRC). By using a variety of signal processing algorithms, the adaptive antenna system can continuously distinguish between the desired signal and the interfering signals and maximize intended signal reception. In an adaptive antenna array system, a DoA for determining the direction of interfering sources is introduced and the adaptive antenna array will steer null patterns towards these interferers. In addition, by using special algorithms and branch diversity techniques, the adaptive antenna array can process and resolve separate multipath signals, which can later be combined. This technique can maximize the signal-to-interference ratio, (S/I) or (signal-to-interference and noise ratio, SINR). Adaptive antenna arrays with N antennas can be regarded as an N-branch diversity scheme, providing more than the traditional two diversity branches. Figure 2.1 shows the block diagram of an adaptive antenna array system.

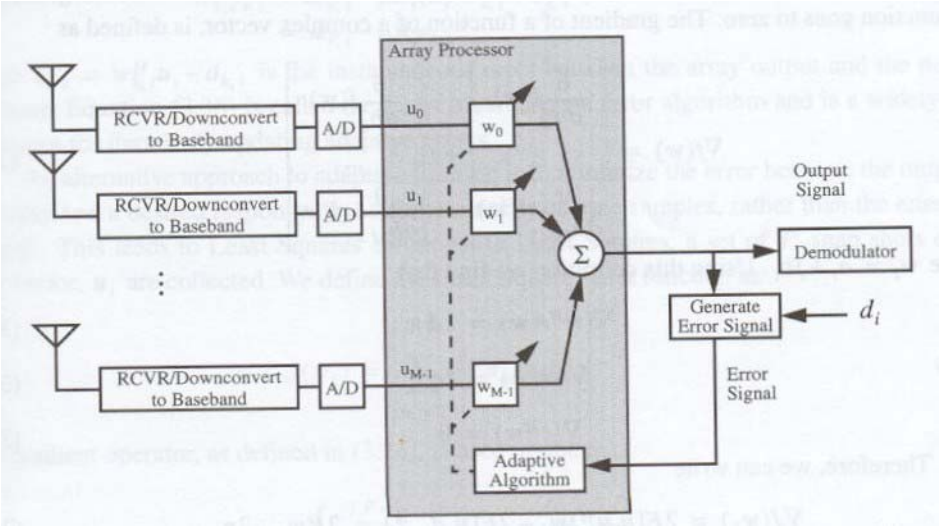

Figure 2.1. Block diagram of an adaptive antenna array system. (From:10).

The RF signals from the N antenna elements are coherently down-converted to an IF frequency, low enough for quality digitization of the signals. The beamformer then processes the digital outputs for each channel by adjusting the amplitude and phase of the signals through the adjustment of the weights with which the signal will be multiplied. This will result in beam and null steering. The adaptive antenna system can be viewed as a spatial filter in which the pass and stop band is created along the direction of the signal and interferers respectively.

For a four-element (N=4) beamformer, there are four antenna output ports receiving each radio channel. For example, in a particular CDMA channel, the beamformer can steer a beam to a desired mobile signal and null to up to three (N-1) interferers sharing that channel. In the case of CDMA, these three interferers are co-channel signals. However in TDMA and FDMA systems, these may be interference transmitted from other users on the same re-use channels in different cells.

The null depth of each interferer will be dependent on the geometry scenario between the various signals. A digitally adaptive beamformer first works to minimize the

signal-to-interference noise ratio (SINR), thereby canceling as many interferers as possible to pass the desired signal with minimum distortion. This is termed null steering. Figure 2.2 illustrates the null steering concept. By varying the desired user direction, ϕ_0, the beam can be steered to any desired direction by adjusting the weighting element, w_m, both in magnitude and phase, and placing a null to the interferers' direction.

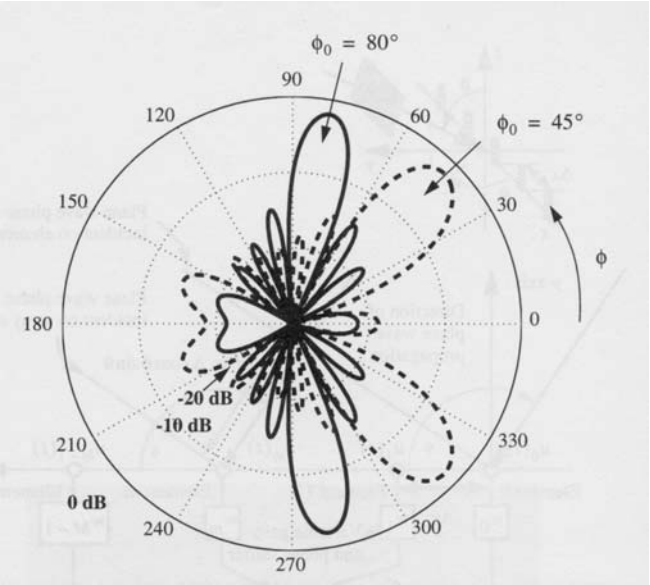

Figure 2.2. Plot of the array factor for the desired user in direction $\phi_0 = 45°$ and $80°$. (From:10).

After this has been achieved, the beamformer uses the remaining degrees of freedom to steer the desired beam towards the source to maximize the background signal-to-noise ratio (SNR). This is termed as beam steering. The greatest advantage of DAB is the high interference rejection potential. This allows maximum improvement of SINR for each subscriber. In this thesis, the adaptive antenna array system will be discussed and its performance will be analyzed.

The next generation of mobile communications, the 'third-generation' (3G) systems, will provide new wideband multimedia and Internet services. These systems build on the investment already made in the current second-generation systems infrastructure. The requirements of these 3G systems far exceed those of the 2G systems and can be satisfied by employing a flexible air interface. There are two possible paths

from present 2G to 3G systems, a GSM/TDMA path and a CDMA path. The chosen system will have to meet a number of criteria as follows:

- Capacity – support for the increased level of voice and data traffic
- Hardware – low cost, compact and power efficient mobile terminals and base stations
- Flexibility – support for a wide range of voice and data services requiring varying bit rates

Smart antennas are regarded as one of the components in the 3G systems. There is considerable interest in the application of smart antenna technology forming an integral part of these next generation systems. The 3G systems proposed will include, other than the ordinary 2G pilot, a diversity pilot, an auxiliary pilot, an auxiliary diversity pilot, and a dedicated pilot. The switched, spot beams and adaptive antenna arrays, and will provide an increase in capacity and performance benefits [5]. It has been shown that adaptive antennas can alleviate the problems, which emerge in 3G direct-sequence code-division multiple access (DS-CDMA,popularly known as wideband CDMA, WCDMA), mixed cell structure. The system offer advantages such as better performance against the near-far effect, more efficient hand over, ability to support high data rates and better coverage in problematic areas. In the 3G systems, fixed spot beams can be generated to increase capacity or coverage in a specific geographic area. In such a case, the spot beam is not associated with a specific user and does not track a user as he moves through the coverage area. However, a spot beam can be directed at a user using the dedicated pilot if he enters an area having poor coverage and the beam is steered as the user moves through the coverage area. This thesis will study and analyze the performance of an adaptive antenna array and the effects of channel coding and RAKE receiver will be considered.

THIS PAGE INTENTIONALLY LEFT BLANK

III. ADAPTIVE ANTENNA ARRAY

As mentioned in Chapter II, the adaptive antenna array is a smart antenna which can maximize the signal-to-interference-plus-noise ratio (SINR) and provide the maximum discrimination against interfering signals by adjusting the weights with which the signals are multiplied.

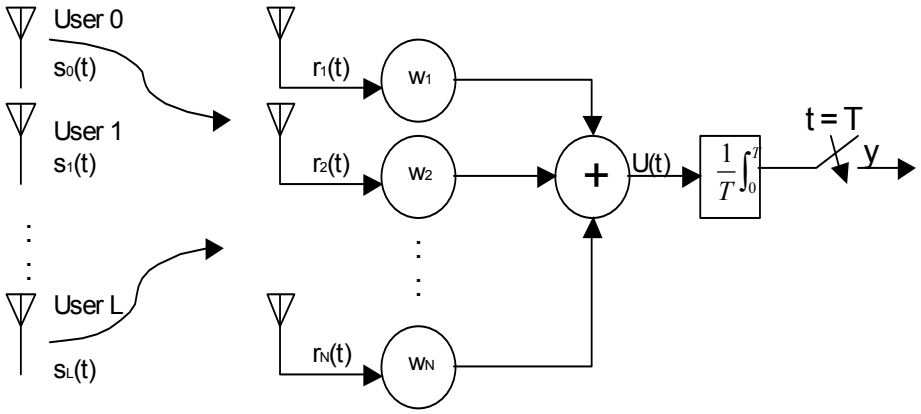

Figure 3.1. Adaptive antenna array with N elements and $L+1$ users.

A. OPTIMAL WEIGHTS FOR NARROWBAND SIGNAL

Figure 3.1 shows an adaptive antenna array having N elements with L interferers which operates in an environment where there is a desired signal with a transmitted complex envelop $s_0(t)$. All signals are assumed to be narrowband and subject to flat Rayleigh fading at each antenna element. It is assumed that the transmitted signals are BPSK signals which satisfies $E_T(|s_i(t)|^2) \equiv \frac{1}{T}\int_{-T/2}^{T/2}|s_i(t)|^2\,dt = 1$ and $i = 0,\cdots,L$. E_T is the time expectation or time averaging operator in the sense of the above integral taken over the symbol period of T which is assumed much smaller than the reciprocal of the fading

rate. All of the random processes involved are assumed to be ergodic so that the ensemble average may be replaced with the time average as required. We assume that the desired and interfering signals are uncorrelated, ie. $E_T[s_i(t)s_k^*(t)] = 0, \text{for } i \neq k \text{ and } i,k = 0,\cdots,L$. From [3] and [4], the complex baseband signal received by the k^{th} branch, $r_k(t)$ is multiplied by an adjustable weight w_k and the weighted signals are summed to form the output signal $u(t)$ as shown below:

$$r_k(t) = \sqrt{P_0}\,\alpha_{0k}\,e^{-j\phi_{ok}}\,s_0(t) + \sum_{i=1}^{L}\sqrt{P_i}\,\alpha_{ik}\,e^{-j\phi_{ik}}\,s_i(t) + n_k(t) \tag{3.1}$$

$$\begin{aligned} u(t) &= \sum_{k=1}^{N} w_k r_k(t) \\ &= \sqrt{P_0}\,s_0(t)\sum_{k=1}^{N} w_k\alpha_{0k}\,e^{-j\phi_{ok}} + \sum_{i=1}^{L}\sqrt{P_i}\,s_i(t)\sum_{k=1}^{N} w_k\alpha_{ik}\,e^{-j\phi_{ik}} + \sum_{k=1}^{N} w_k n_k(t) \\ &= s_0(t)\mathbf{w}^{+}\mathbf{v}_0 + \sum_{i=1}^{L} s_i(t)\mathbf{w}^{+}\mathbf{v}_i + \mathbf{w}^{+}\mathbf{n}(t) \\ &= \mathbf{w}^{+}\mathbf{r}(t) \end{aligned} \tag{3.2}$$

where $^{+}$ denotes the Hermitian transpose (which is transpose and complex conjugate) and

$$\mathbf{w} = [w_1\ w_2\ \cdots\ w_N]^T$$

$$\mathbf{v}_i = \sqrt{P_i}\begin{bmatrix} \alpha_{i1}e^{-j\phi_{i1}} \\ \alpha_{i1}e^{-j\phi_{i1}} \\ \vdots \\ \alpha_{iN}e^{-j\phi_{iN}} \end{bmatrix} \qquad i = 0,1,\cdots L$$

$$\mathbf{n}(t) = \begin{bmatrix} n_0(t) \\ \vdots \\ n_N(t) \end{bmatrix}$$

The total array input in the presence of additive noise is:

$$\mathbf{r}(t) = s_0(t)\mathbf{v}_0 + \sum_{i=1}^{L} s_i(t)\mathbf{v}_i + \mathbf{n}(t)$$

where ***n(t)*** is the noise vector at the input of the array and the vector $\mathbf{v}_{i,}\ i = 0,1,\cdots L$ is the propagation vector of the i^{th} user.

The array output, *y*, after the integrator, can be defined as:

$$y = \frac{1}{T}\int_0^T u(t)dt \tag{3.3}$$

Hence,

$$y = \pm\mathbf{w}^{+}\mathbf{v}_0 + \sum_{i=1}^{L}\left[\frac{1}{T}\int_o^T s_i(t)dt\right]\mathbf{w}^{+}\mathbf{v}_i + \mathbf{w}^{+}\left[\frac{1}{T}\int_o^T \mathbf{n}(t)dt\right] \tag{3.4}$$

From [4], the optimum weights can be obtained by using the minimum mean square error (MMSE) criterion and are given as:

$$\mathbf{W}_{opt} = \alpha\mathbf{\Phi}_{nI}^{-1}\mathbf{v}_0 \tag{3.5}$$

where $\mathbf{\Phi}_{nI} = \sum_{i=1}^{L} v_{ik}v_{ik}^{+} + \sigma^2 I_N$ is the short term noise-plus-interference correlation matrix as defined in [4] and α is some proportionality constant. Since the SINR is insensitive to modifying the weights by a scaling factor, the factor α can be omitted without loss of generality.

B. OUTPUT SIGNAL-TO-NOISE PLUS INTERFERENCE RATIO (SINR)

Similarly, the instantaneous output SINR, γ, has been defined in equation (8.71) of [4] as:

$$\gamma_{opt} = \mathbf{v}_0^{+}\mathbf{w}_{opt} = \mathbf{v}_0^{+}\mathbf{\Phi}_{nI}^{-1}\mathbf{v}_0 \tag{3.6}$$

where $\mathbf{W}_{opt} = \mathbf{\Phi}_{nI}^{-1}\mathbf{v}_0$

C. STATISTIC OF THE OUTPUT SINR

The PDF and CDF of the optimized output SINR without coding has been derived in [3] and [4]. Since the propagation vectors $\mathbf{v}_i$, are complex Gaussian, the multivariate PDF of $\mathbf{v}_i$, $p_i(\mathbf{v}_i)$, for Rayleigh fading is :

$$p_i(\mathbf{v}_i) = \frac{1}{(\pi)^N \mid \mathbf{R}_i \mid} \exp(-\mathbf{v}_i^{+} \mathbf{R}_i^{-1} \mathbf{v}_i), \qquad i = 0, ..., L \tag{3.7}$$

where $\mid \mid$ denotes determinant and $\mathbf{R}_i$ is the normalized correlation matrix corresponding to the propagation vector of the i^{th} user. This definition is possible because $\mathbf{R}_i$ is Hermitian. Since the signals from various users are assumed to have independent fadings, the joint density function of $\mathbf{v}_1, \ldots, \mathbf{v}_L$ is given by

$$p_v(\mathbf{v}_0, \cdots, \mathbf{v}_L) = \prod_{i=0}^{L} p_i(\mathbf{v}_i) \tag{3.8}$$

The PDF of the output SINR can be found by first determining its characteristic function through the Laplace transform

$$\begin{aligned} \Psi(s) &= \int_0^{\infty} p(\gamma) \exp(-s\gamma) d\gamma \\ &= \langle \exp(-s\gamma) \rangle \end{aligned} \tag{3.9}$$

where $\langle . \rangle$ denotes the overall statistical average over all users. Note that $\gamma \geq 0$, i.e. $p(\gamma) = 0$ for $\gamma < 0$, so

$$\begin{aligned} \Psi(s) &= \langle \exp(-s\gamma) \rangle \\ &= \int_{-\infty}^{\infty} \cdots \int_{-\infty}^{\infty} p_v(\mathbf{v}_0, \cdots, \mathbf{v}_L) \exp(-s\mathbf{v}_0^{+} \mathbf{\Phi}_{nI}^{-1} \mathbf{v}_0) \, d\mathbf{v}_0 \cdots d\mathbf{v}_L \\ &= \int_{-\infty}^{\infty} \cdots \int_{-\infty}^{\infty} p_1(\mathbf{v}_1), \cdots, p_L(\mathbf{v}_L) \, d\mathbf{v}_0 \cdots d\mathbf{v}_L \cdots G(s, \mathbf{v}_1 \cdots \mathbf{v}_L) \end{aligned} \tag{3.10}$$

where

$$
\begin{aligned}
G(s,\mathbf{v}_1\cdots\mathbf{v}_L) &= \int_{-\infty}^{\infty} p_0(\mathbf{v}_0)\exp(-s\mathbf{v}_0^{+}\boldsymbol{\Phi}_{nI}^{-1}\mathbf{v}_0)\,d\mathbf{v}_0 \\
&= \frac{1}{\pi^N\,|\,\mathbf{R}_0\,|}\int_{-\infty}^{\infty}\exp[-\mathbf{v}_0^{+}(\mathbf{R}_0^{-1}+s\boldsymbol{\Phi}_{nI}^{-1})\mathbf{v}_0]\,d\mathbf{v}_0 \\
&= \frac{1}{\pi^N\,|\,\mathbf{R}_0\,|}\frac{\pi^N}{|\,\mathbf{R}_0^{-1}+s\boldsymbol{\Phi}_{nI}^{-1}\,|} \\
&= \frac{1}{|\,\mathbf{I}_N+s\mathbf{R}_0\boldsymbol{\Phi}_{nI}^{-1}\,|}
\end{aligned}
\tag{3.11}
$$

Since the determinant of a matrix can be written in terms of the product of its eigenvalues, we can write

$$
G(s,\mathbf{v}_1,\cdots,\mathbf{v}_L) = G(s,\lambda_1,\cdots,\lambda_N) = \prod_{n=1}^{N}\frac{1}{1+\frac{s}{\lambda_n}} \tag{3.12}
$$

where $\lambda_1,\cdots,\lambda_N$ are the eigenvalues of $(\mathbf{R}_0\boldsymbol{\Phi}_{nI}^{-1})^{-1} = \boldsymbol{\Phi}_{nI}\mathbf{R}_0^{-1}$. They are the solution to the general eigenvalue problem

$$
\boldsymbol{\Phi}_{nI}u = \lambda\mathbf{R}_0u. \tag{3.13}
$$

The characteristic function given in [3] and [4] is just the expectation of $G(s,\lambda_1,\cdots,\lambda_N)$ with respect to $\lambda_1,\cdots,\lambda_N$

$$
\Psi(s) = \langle G(s,\lambda_1,\cdots,\lambda_N)\rangle \tag{3.14}
$$

In general, it is extremely difficult to evaluate the characteristic function exactly by carrying out the expectation operator on (3.12). An estimate of $\Psi(s)$ can be made by using the usual technique of expanding $G(s,\lambda_1,\cdots,\lambda_N)$ in a Taylor series from which $\Psi(s)$ can be expressed in terms of the mean, covariance and higher moments of

$\lambda_1, \cdots, \lambda_N$ [6]. The first order approximation itself was shown in [3] to yield accurate results in most cases. Thus

$$\Psi(s) \cong \prod_{n=1}^{N} \frac{1}{1+\frac{s}{\langle \lambda_n \rangle}} = \prod_{n=1}^{N} \frac{\langle \lambda_n \rangle}{s+\langle \lambda_n \rangle} \tag{3.15}$$

The mean eigenvalues $\langle \lambda_n \rangle$ are all real and positive due to positive definite and Hermitian nature of $\mathbf{\Phi}_{nI}$ and $\boldsymbol{R}_0$. The PDF of the output SINR can be determined by an inverse Laplace transform of $\Psi(s)$. Assuming that there are M distinct eigenvalues, $M \leq N$, and one eigenvalue of multiplicity $(N\text{-}M)$ in the most general case of interest, the characteristic function can be expressed as a partial fraction expansion

$$\Psi(s) = \sum_{i=1}^{M} \frac{B_i}{s+\langle \lambda_i \rangle} + \sum_{i=1}^{N-M} \frac{C_i}{(s+\langle \lambda_N \rangle)^i} \tag{3.16}$$

where

$$B_i = \lim_{s \to -\langle \lambda_i \rangle} \{\Psi(s)(s+\langle \lambda_i \rangle)\} \tag{3.17}$$

and

$$C_i = \frac{1}{(N-M-i)!} \lim_{s \to -\langle \lambda_N \rangle} \left(\frac{d}{ds} \right)^{N-M-i} \{\Psi(s)(s+\langle \lambda_N \rangle)^{N-M}\} \tag{3.18}$$

Taking the inverse Laplace transform of $\Psi(s)$ yields the PDF

$$\begin{aligned} p(\gamma) &= L^{-1}\{\Psi(s)\} \\ &= \sum_{i=1}^{M} B_i e^{-\gamma \langle \lambda_i \rangle} + \sum_{i=1}^{N-M} C_i \frac{\gamma^{i-1}}{(i-1)!} e^{-\gamma \langle \lambda_N \rangle} \end{aligned} \tag{3.19}$$

The CDF of the output SINR is therefore:

$$\begin{aligned} P(\gamma) &= \int_0^{\gamma} p(\mu) d\mu \\ &= \sum_{i=1}^{M} \frac{B_i}{\langle \lambda_i \rangle} \left[1 - e^{-\gamma \langle \lambda_i \rangle} \right] + \sum_{i=1}^{N-M} \frac{C_i}{\langle \lambda_N \rangle^i} \left[1 - \sum_{k=0}^{i-1} \frac{\gamma^k \langle \lambda_N \rangle^k}{k!} e^{-\gamma \langle \lambda_N \rangle} \right] \end{aligned} \tag{3.20}$$

From page 253 of [4], under the first order approximation, the statistics of the output SINR are specified in terms of the mean eigenvalues of (3.13). Hence the mean output SINR of the array can be determined to be

$$\Gamma_N = \sum_{n=1}^{N} \left\langle \frac{1}{\lambda_n} \right\rangle \approx \sum_{n=1}^{N} \frac{1}{\langle \lambda_n \rangle}. \tag{3.21}$$

Now, assume that the antenna elements have the same gain and are separated by sufficiently large spacing (in terms of operating wavelength) such that the branch signals are uncorrelated. Then the covariance matrix of the signals can be written as

$$\mathbf{R}_j = \mathbf{P}_j \mathbf{I}_N, \qquad 0 \le j \le L \tag{3.22}$$

where

$$\mathbf{P}_j = \left\langle \mathbf{v}_{ji} \mathbf{v}_{ji}^* \right\rangle, \quad 1 \le i \le N \tag{3.23}$$

is the average received j^{th} signal power at the i^{th} branch and P_0 is the total amount of power received from the desired user. In the presence of thermal noise and multiple interferers, the short-term noise-plus-interference covariance matrix is given by

$$\mathbf{\Phi}_{nI} = \mathbf{\Phi}_I + \sigma^2 \mathbf{I}_N \tag{3.24}$$

where $\mathbf{\Phi}_I = \sum_{i=1}^{L} \mathbf{v}_{ik} \mathbf{v}_{ik}^{+}$ is the N x N short term interference covariance matrix for multiple interferers.

The generalized eigenvalue problem (3.13) becomes

$$(\sigma^2 \mathbf{I}_N + \mathbf{\Phi}_I) u_n = \lambda \mathbf{P}_0 u_n \tag{3.25}$$

which can be written as

$$\mathbf{\Phi}_I u_n = (\lambda \mathbf{P}_0 - \sigma^2) u_n = \alpha_n u_n \tag{3.26}$$

where

$$\alpha_n = \lambda P_0 - \sigma^2 \tag{3.27}$$

are the eigenvalues of $\mathbf{\Phi}_I$, which is an N x N matrix of rank L with L non-zero eigenvalues. Assuming that the interferers are all of equal strength so that the received power $P_j = P_1, j = 2,...,L$ and writing $\alpha_n = a_n P_1$, where a_n are the normalized mean eigenvalues as defined in [3] are shown in Table 3.1 for several values of N and L. The signal-to-noise ratios for the desired signal and each interference signal are defined as

$$\Gamma_0 = \frac{P_0}{\sigma^2} \qquad \text{and} \qquad \Gamma_1 = \frac{P_1}{\sigma^2}.$$

It follows that

$$\langle \lambda_n \rangle = \frac{\langle \alpha_n \rangle + \sigma^2}{P_0} = \frac{a_n \Gamma_1 + 1}{\Gamma_0}, \quad 1 \le n \le N \tag{3.28}$$

$$\Gamma_N = N \Gamma_0 \left[1 - \frac{\Gamma_1}{N} \sum_{n=1}^{N} \frac{a_n}{1 + a_n \Gamma_1} \right]. \tag{3.29}$$

The mean input SINR at each branch is

$$\Gamma = \frac{P_0}{\sum_{j=1}^{L} P_j + \sigma^2} = \frac{\Gamma_0}{\sum_{j=1}^{L} \Gamma_j + 1}. \tag{3.30}$$

It is noted that the mean output SINR of the array is less than $N\Gamma_0$, which is the value obtained with a maximal ratio combiner (MRC) without any interferers, ie. $\Gamma_1 = 0$.

	L=1	**2**	**3**	**4**	**5**
N=1	1.00	2.00	3.00	4.00	5.00
2	0.00	0.50	1.12	1.81	2.54
	2.00	3.50	4.88	6.19	7.46
3	0.00	0.00	0.33	0.79	1.32
	0.00	1.12	2.15	3.16	4.16
	3.00	4.88	6.52	8.05	9.52
4	0.00	0.00	0.00	0.25	0.61
	0.00	0.00	0.79	1.57	2.37
	0.00	1.81	3.16	4.41	5.63
	4.00	6.19	8.05	9.77	11.39
5	0.00	0.00	0.00	0.00	0.20
	0.00	0.00	0.00	0.61	1.24
	0.00	0.00	1.32	2.37	3.39
	0.00	2.54	4.16	5.63	7.01
	5.00	7.46	9.52	11.39	13.16

Table 3.1. Intrinsic Mean Eigenvalues, $a_i = \langle \alpha_i \rangle / P_i$ (From:3).

D. BER PERFORMANCE FOR OPTIMUM COMBINING

The average bit error rate (BER) performance of basic modulation schemes can be found by taking the expectation of the conditional bit error rate as defined

$$BER = \int_0^\infty P_e(\gamma) p(\gamma) d\gamma \tag{3.31}$$

where $P_e(\gamma)$ is the conditional bit error rate and $p(\gamma)$ is the PDF of the output SINR without coding.

For BPSK signals, $P_e(\gamma) = Q(\sqrt{2\gamma}) = \frac{1}{2}\text{erfc}(\sqrt{\gamma})$, the BER performance for optimum combining with multiple interferers using an adaptive array without coding is given in [3] as

$$\begin{aligned} BER &= \int_0^\infty P_e(\gamma) p(\gamma) d\gamma \\ &= \int_0^\infty \left(\sum_{i=1}^{M} B_i e^{-\gamma\langle\lambda_i\rangle} + \sum_{i=1}^{N-M} C_i \frac{\gamma^{i-1}}{(i-1)!} e^{-\gamma\langle\lambda_N\rangle} \right) Q(\sqrt{2\gamma}) d\gamma. \end{aligned} \tag{3.32}$$

Using the general integral formula [7]:

$$\frac{1}{2(K-1)} \int_0^\infty x^{K-1} e^{-ax} \text{erfc}(\sqrt{bx}) dx = \left(\frac{\sqrt{1+\frac{a}{b}}-1}{2a\sqrt{1+\frac{a}{b}}} \right)^K \sum_{k=1}^{K-1} \binom{K-1+k}{k} \left(\frac{\sqrt{1+\frac{a}{b}}+1}{2\sqrt{1+\frac{a}{b}}} \right)^k \tag{3.33}$$

we obtain

$$BER = \sum_{i=1}^{M} B_i \mu_i + \sum_{i=1}^{N-M} C_i \mu_N^i \sum_{k=0}^{i-1} \binom{i+k-1}{k} \beta^k \tag{3.34}$$

where

$$\mu_i = \frac{\sqrt{1+\langle\lambda_i\rangle}-1}{2\langle\lambda_i\rangle\sqrt{1+\langle\lambda_i\rangle}}$$

$$\beta = \frac{\sqrt{1+\langle\lambda_N\rangle}+1}{2\sqrt{1+\langle\lambda_N\rangle}}$$

Figure 3.2 shows the plot of BER performance of BPSK versus the average branch SINR of an adaptive antenna with several uncorrelated branches and 2 interferers (L=2) of equal strength with $\Gamma_1 = 2$ (which is 3 dB). From the plot, it can be seen that the BER is exactly the same as in [3] and [4]. When the number of elements is increased from 3 to 5, it is seen that the bit error rate is significantly reduced, due mainly to the diversity gain. Note that the mean eigenvalues in (3.34) can be expressed in terms of Γ_1 and Γ as

$$\langle \lambda_n \rangle = \frac{a_n \Gamma_1 + 1}{\Gamma(L\Gamma_1 + 1)} \tag{3.35}$$

where a_n is given in Table 3.1, and L is the number of interferers which is set to 2.

Figure 3.3 shows the plot of BER performance of BPSK versus the total SNR of adaptive antenna without coding effect. The total input SNR, $N\Gamma_0$ is expressed as a function of average input SINR, Γ from (3.30). Figure 3.4 compares the BER performance for different total signal-to-interference ratio (SIR) and it is obtained by using the following expression:

$$\langle \lambda_n \rangle = \frac{\langle \alpha_n \rangle + \sigma^2}{P_0} = \frac{a_n P_1 + 1}{P_0} = \frac{a_n}{\gamma_1} + \frac{1}{\Gamma_0}, \qquad 1 \le n \le N \tag{3.36}$$

where $\gamma_1 = \frac{P_0}{P_1}$ is the signal-to-interference power ratio (SIR) of interferer 1 and $\Gamma_I = \sum_{j=1}^{L} \gamma_j$ is the total SIR per bit. Here, we assume that the SIRs of all interferers are the same, ie. $\gamma_j = \gamma_{1,} j = 2,...,L$ and $\Gamma_I = L\gamma_1$.

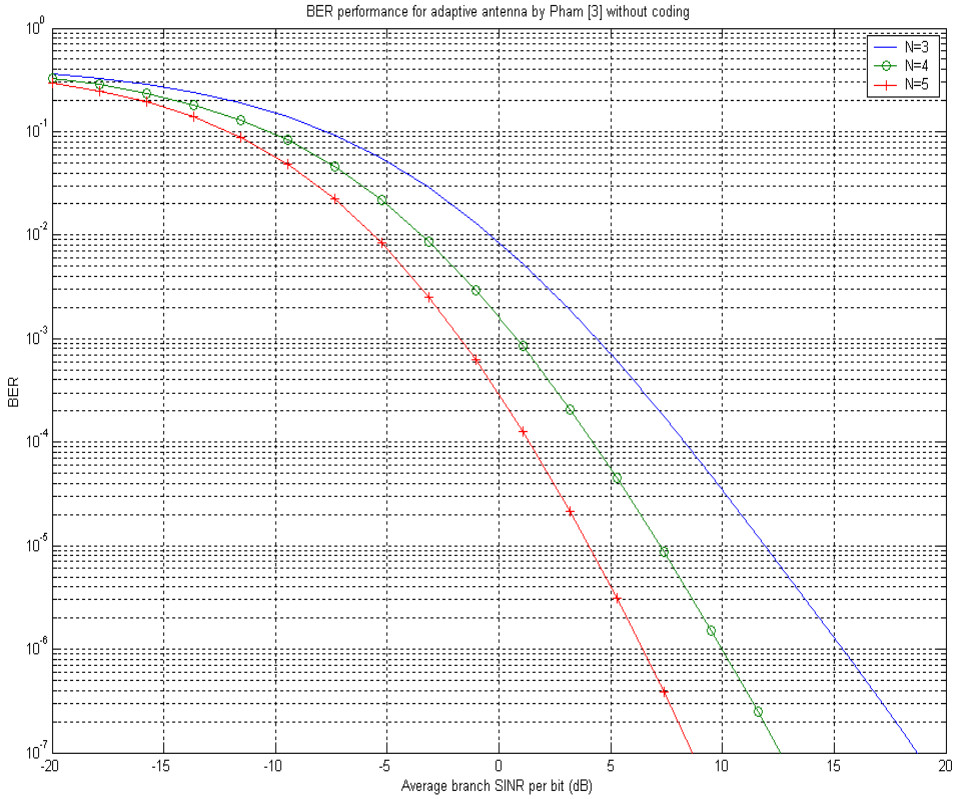

Figure 3.2. BER performance of BPSK versus the average branch SINR per bit of adaptive antenna without coding effect (*L=2,* $\Gamma_1 = \Gamma_2 = 3\,\text{dB}$*).*

In the absence of interference, the undesired signals consists only of thermal noise, and thus are uncorrelated between branches, ie. $\mathbf{\Phi}_{nI} = \sigma^2 \mathbf{I}_N$. In this case, the weights become $\mathbf{w}_{opt} = \frac{\mathbf{v}_0}{\sigma^2}$ and the output SINR, $\gamma_{opt} = \mathbf{v}_0{}^{+}\mathbf{w}_{opt} = \frac{\mathbf{v}_0{}^{+}\mathbf{v}_0}{\sigma^2}$. Hence, the adaptive array reduces to a Maximal Ratio Combiner (MRC). The generalized eigenvalue problem (3.13) is reduced to

$$\sigma^2 \mathbf{I}_N u = \lambda \mathbf{R}_0 u. \tag{3.37}$$

which is a deterministic problem where the eigenvalue is

$$\langle \lambda \rangle = \frac{\sigma^2}{R_0} = \frac{\sigma^2}{P_0} = \frac{1}{\Gamma_0} \tag{3.38}$$

The characteristic function in (3.15) will be changed to,

$$\Psi(s) = \prod_{n=1}^{N} \frac{\langle \lambda \rangle}{s + \langle \lambda \rangle} = \left[\frac{\langle \lambda \rangle}{s + \langle \lambda \rangle} \right]^N = \sum_{i=1}^{N} \frac{A_i}{(s + \langle \lambda \rangle)^i} \tag{3.39}$$

where

$$A_i = \frac{1}{(N-i)!} \lim_{s \to -\langle \lambda \rangle} \left(\frac{d}{ds} \right)^{N-i} \{ \Psi(s)(s + \langle \lambda \rangle)^N \} \tag{3.40}$$

Again, the PDF can be found by taking the inverse Laplace transform of $\Psi(s)$,

$$\begin{aligned} p(\gamma) &= L^{-1}\{\Psi(s)\} \\ &= \sum_{i=1}^{N} A_i \frac{\gamma^{i-1}}{(i-1)!} e^{-\gamma \langle \lambda \rangle} \end{aligned} \tag{3.41}$$

The BER performance of MRC with Rayleigh fading can be determined as follows:

$$\begin{aligned} BER &= \frac{1}{2} \int_0^\infty p(\gamma) \operatorname{erfc}(\sqrt{\gamma}) d\gamma \\ &= \frac{1}{2} \int_0^\infty \left[\sum_{i=1}^{N} A_i \frac{\gamma^{i-1}}{(i-1)!} e^{-\gamma \langle \lambda \rangle} \right] \operatorname{erfc}(\sqrt{\gamma}) d\gamma. \end{aligned} \tag{3.42}$$

Again, using the general integral formula in equation (3.33),

$$BER = \sum_{i=1}^{N} A_i \left[\frac{\sqrt{1+\langle\lambda\rangle}-1}{2\langle\lambda\rangle\sqrt{1+\langle\lambda\rangle}} \right]^i \sum_{k=0}^{i-1} \binom{i+k-1}{k} \left[\frac{\sqrt{1+\langle\lambda\rangle}+1}{2\sqrt{1+\langle\lambda\rangle}} \right]^k \tag{3.43}$$

The BER performance of BPSK versus the total SNR per bit for Maximum Ratio Combining (MRC) with several uncorrelated branches is shown in Figure 3.5. The BER plot is seen to be same as the BER plot in Figure 7.8 of [4], page 201, which shows that the equation (3.43) is equivalent to equation (7.44) of [4]. Similarly, by comparing BER plot in Figure 3.3 with that of Figure 14.4-2 of [8], it is also seen that the BER plot is exactly the same, which implies that equation (3.43) is equivalent to equation (14.4-15) in [8]. The performance of the adaptive antenna acting as MRC improves greatly as the number of antenna elements increases.

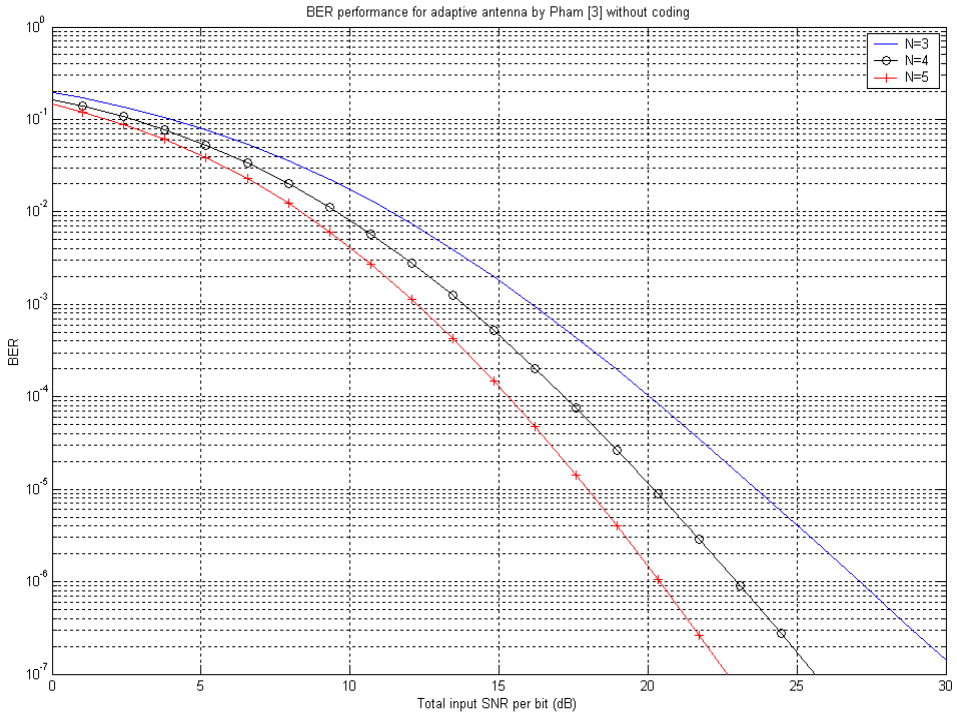

Figure 3.3. BER performance of BPSK versus the total SNR per bit of adaptive antenna without coding effect (*L=2,* $\Gamma_1 = \Gamma_2 = 3\,\text{dB}$*)*.

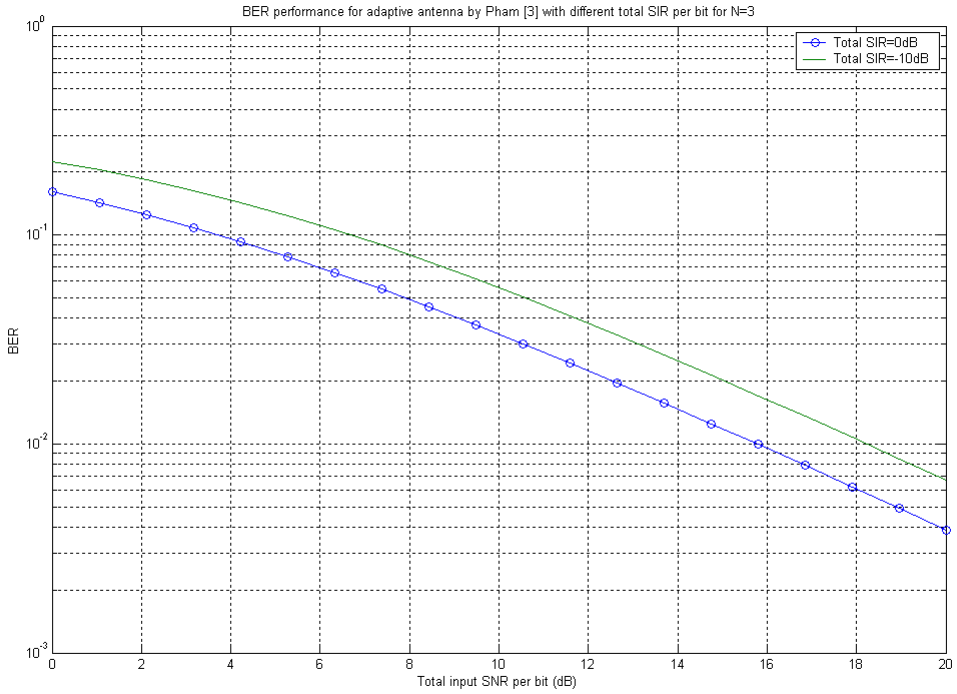

Figure 3.4. BER performance of BPSK versus the total SNR of adaptive antenna without coding effect and different value of total SIR (*L=2,* $\Gamma_I = L\gamma_1 = 0\,\text{dB}$ or $-10\,\text{dB}$*)*.

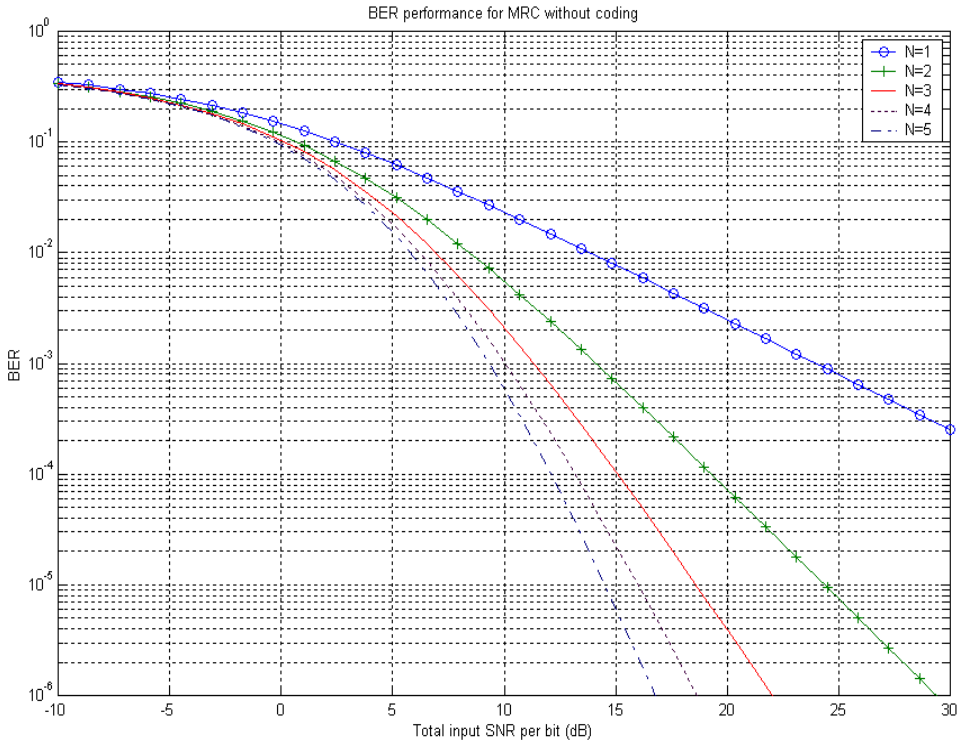

Figure 3.5. BER performance of BPSK versus the total SNR per bit for Maximum Ratio Combining (MRC) without coding.

IV. FORWARD ERROR CORRECTION

As mentioned in Chapter II, the adaptive antenna array is a smart antenna which can maximize the signal-to-interference-plus-noise ratio (SINR) and provide the maximum discrimination against interfering signals by adjusting the weights with which the signals are multiplied. The system performance improvement by the adaptive antenna is due to the spatial diversity effect. To further improve the performance of the communication link, forward error correction (FEC) in the form of convolutional codes can be exploited. In a (n,k) convolutional encoder, n coded bits are transmitted for every k information bits and the code rate is given by $R_c = k/n$. In order to preserve the bit rate of the system, the bit duration for the coded system is reduced to $T_c=T_bR_c=T(k/n)$. The convolutional encoder has a constraint length of v, which means that a single information bit can affect the output of the encoder for a maximum of v shifts, as defined in [8]. Therefore, at least one of the k shift registers that make up the encoder has a length of (v-1).

Channel coding protects digital data from errors by selectively introducing redundancies in the transmitted data and it allows the receiver to detect and correct errors, thereby improving the system performance.

A. OUTPUT SIGNAL-TO-NOISE PLUS INTERFERENCE RATIO

Figure 4.1 is similar to Figure 3.1 (which shows an adaptive antenna array having N elements with L interferers) except that a Viterbi soft decoder is now included. Again, all signals are assumed to be narrowband and subject to flat Rayleigh fading at each antenna element.

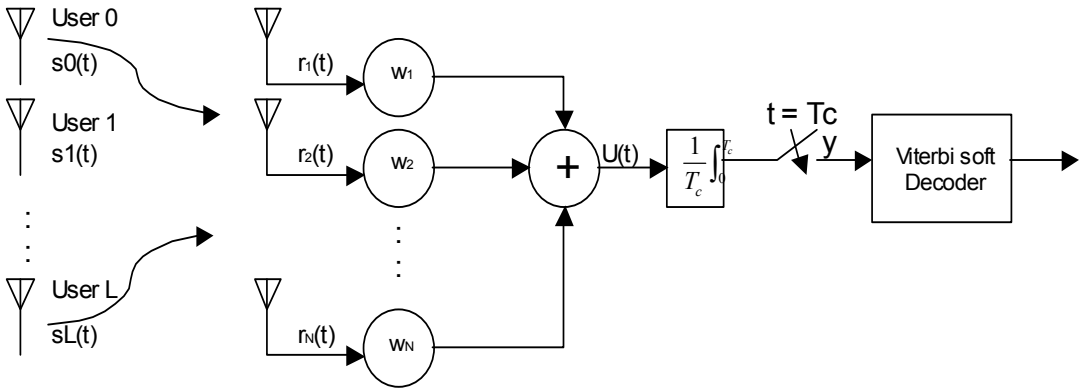

Figure 4.1. Adaptive antenna array with coding.

The probability of error for convolutional codes is derived by employing the linearity property for this class of codes to simplify the derivation [8]. We assume that the all zero code sequence is transmitted and determine the probability of error in deciding in favor of another code sequence. The coded binary bits for the jth branch of the convolutional code, denoted as $\{c_{jm}, j=1,2,...,n;\ m=1,2,...,n\}$, where the index j indicates the jth branch and the index m is the mth bit in that branch of the trellis diagram, are assumed to be transmitted by binary PSK (BPSK) and demodulated coherently.

The Viterbi soft-decision decoder forms the branch metrics defined in equation (8.2-14) by Proakis [8] and the first-event error probability $P_2(d)$ defined in equation (8.2-19) by Proakis [8].

The upper bound on the first-event error probability, P_e can be calculated using the number of information bit errors β_d associated with selecting a path of distance d from the all-zero path as shown in [8]:

$$P_e \le \frac{1}{k} \sum_{d=d_{free}}^{\infty} \beta_d P_2(d). \qquad (4.1)$$

The conditional probability $P_2(d)$ is the probability that the sum of d independent and identically distributed samples y_k at the output of the BPSK demodulator is greater than zero, [8] and [9], that is :

$$P_2(d) = \Pr\left\{\sum_{k=1}^{d} y_k \geq 0\right\}. \tag{4.2}$$

The random variable y_k is given in (3.4) as :

$$y_k = u_{0k}\mathbf{w}_k{}^{+}\mathbf{v}_{0k} + \sum_{i=1}^{L} u_{ik}\mathbf{w}_k{}^{+}\mathbf{v}_{ik} + \mathbf{w}_k{}^{+}\mathbf{n}_k \tag{4.3}$$

where

$$u_{0k} = -1, \qquad u_{ik} = \frac{1}{T_c}\int_{kT_c}^{(k+1)T_c} s_i(t)dt, \qquad n_k = \frac{1}{T_c}\int_{kT_c}^{(k+1)T_c} n(t)dt$$

We also assume the all the transmitted signals have the same property, that is, $E\{u_{ik}{}^2\} = 1$ for all i = 0,1,…L and we let $\sigma^2 = E\{\mathbf{n}_k{}^2\}$. Here, T_c is the coded bit duration. The probability $P_2(d)$ has been derived in [9] as follows:

$$P_2(d) = \frac{1}{2}\operatorname{erfc}(\sqrt{\gamma_d}) \tag{4.4}$$

where γ_d can be viewed as the SINR of the selected distance-d path

$$\gamma_d = \frac{E\{\sum_{k=1}^{d} y_k\}^2}{\operatorname{var}\{\sum_{k=1}^{d} y_k\}} \tag{4.5}$$

From (4.5) above, we get

$$
\begin{aligned}
\gamma_d &= \frac{E\{|\sum_{k=1}^{d} u_{0k} w_k{}^{+} v_{0k}|^2\}}{E\{|\sum_{k=1}^{d}\sum_{i=1}^{L} u_{ik}(t) w_k{}^{+} v_{ik} + \sum_{k=1}^{d} w_k{}^{+} n_k(t)|^2\}} \\
&= \frac{(\sum_{k=1}^{d} w_k{}^{+} v_{0k})(\sum_{k=1}^{d} v_{0k}{}^{+} w_k)}{\sum_{k=1}^{d}\sum_{i=1}^{L} w_k{}^{+} v_{ik} v_{ik}{}^{+} w_k + \sum_{k=1}^{d} w_k{}^{+} \sigma^2 I_N w_k} \\
&= \frac{(\sum_{k=1}^{d} w_k{}^{+} v_{0k})(\sum_{k=1}^{d} v_{0k}{}^{+} w_k)}{\sum_{k=1}^{d}\left[(\sum_{i=1}^{L} w_k{}^{+} v_{ik} v_{ik}{}^{+} w_k) + w_k{}^{+} \sigma^2 I_N w_k \right]} \\
&= \frac{(\sum_{k=1}^{d} w_k{}^{+} v_{0k})(\sum_{k=1}^{d} v_{0k}{}^{+} w_k)}{\sum_{k=1}^{d}\left[w_k{}^{+} (\sum_{i=1}^{L} v_{ik} v_{ik}{}^{+} + \sigma^2 I_N) w_k \right]} \\
&= \frac{(\sum_{k=1}^{d} w_k{}^{+} v_{0k})(\sum_{k=1}^{d} v_{0k}{}^{+} w_k)}{\sum_{k=1}^{d}\left[w_k{}^{+} \Phi_{nI} w_k \right]}
\end{aligned}
\tag{4.6}
$$

where $\mathbf{I}_N = N \text{ x } N$ identity matrix and $\mathbf{\Phi}_{nI} = \sum_{i=1}^{L} \mathbf{v}_{ik} \mathbf{v}_{ik}{}^{+} + \sigma^2 \mathbf{I}_N$ is the short term noise-plus-interference correlation matrix. From [4], page 248, since $\mathbf{w}_{opt} = \mathbf{\Phi}_{nI}{}^{-1} \mathbf{v}_0$ results in $\mathbf{\Phi}_{nI} \mathbf{w}_{opt} = \mathbf{v}_0$, the optimum SINR at output of Viterbi decoder is :

$$
\begin{aligned}
\gamma_d &= \frac{(\sum_{k=1}^{d} \mathbf{w}_{opt}{}^{+} \mathbf{v}_{0k})(\sum_{k=1}^{d} \mathbf{v}_{0k}{}^{+} \mathbf{w}_{opt})}{\sum_{k=1}^{d}\left[\mathbf{w}_{opt}{}^{+} \mathbf{v}_{0k} \right]} \\
&= \sum_{k=1}^{d} \mathbf{v}_{0k}{}^{+} \mathbf{w}_{opt}
\end{aligned}
$$

$$
\gamma_d = \sum_{k=1}^{d} \gamma_k \tag{4.7}
$$

where γ_k is the SINR of a sample y_k. Hence, coding provides d-diversity order as seen in (4.7)

B. STATISTIC OF THE OUTPUT SINR

Using the same approach as in Chapter III C, the characteristic function of the PDF of γ_d can be extended from (3.15) as

$$\Psi_d(s) = \prod_{n=1}^{N}\left(\frac{\langle\lambda_n\rangle}{s+\langle\lambda_n\rangle}\right)^d = \left(\frac{\langle\lambda_1\rangle}{s+\langle\lambda_1\rangle}\right)^d\left(\frac{\langle\lambda_2\rangle}{s+\langle\lambda_2\rangle}\right)^d\cdots\left(\frac{\langle\lambda_N\rangle}{s+\langle\lambda_N\rangle}\right)^d \tag{4.8}$$

Again, the PDF of the output SINR can be determined by an inverse Laplace transform of $\Psi_d(s)$. Assuming that there are M distinct eigenvalues, $M \le N$, and one eigenvalue of multiplicity (N-M) in the most general case of interest, the characteristic function can be expressed as a partial fraction expansion

$$\begin{aligned}\Psi_d(s) &= \left[\prod_{n=1}^{M}\left(\frac{\langle\lambda_n\rangle}{s+\langle\lambda_n\rangle}\right)^d\right]\left(\frac{\langle\lambda_N\rangle}{s+\langle\lambda_N\rangle}\right)^{(N-M)d} \\ &= \sum_{i=1}^{d}\frac{A_{i1}}{(s+\langle\lambda_1\rangle)^i} + \sum_{i=1}^{d}\frac{A_{i2}}{(s+\langle\lambda_2\rangle)^i} + \cdots + \sum_{i=1}^{d}\frac{A_{iM}}{(s+\langle\lambda_M\rangle)^i} + \sum_{k=1}^{(N-M)d}\frac{A_{kN}}{(s+\langle\lambda_N\rangle)^k} \\ &= \sum_{i=1}^{d}\left[\frac{A_{i1}}{(s+\langle\lambda_1\rangle)^i} + \frac{A_{i2}}{(s+\langle\lambda_2\rangle)^i} + \cdots + \frac{A_{iM}}{(s+\langle\lambda_M\rangle)^i}\right] + \sum_{k=1}^{(N-M)d}\frac{A_{kN}}{(s+\langle\lambda_N\rangle)^k}\end{aligned} \tag{4.9}$$

where

$$
\begin{aligned}
A_{i1} &= \frac{1}{(d-i)!}\lim_{s\to-\langle\lambda_1\rangle}\left(\frac{d}{ds}\right)^{d-i}\{\Psi_d(s)(s+\langle\lambda_1\rangle)^d\} \\
A_{i2} &= \frac{1}{(d-i)!}\lim_{s\to-\langle\lambda_2\rangle}\left(\frac{d}{ds}\right)^{d-i}\{\Psi_d(s)(s+\langle\lambda_2\rangle)^d\} \\
&\vdots \\
A_{iM} &= \frac{1}{(d-i)!}\lim_{s\to-\langle\lambda_M\rangle}\left(\frac{d}{ds}\right)^{d-i}\{\Psi_d(s)(s+\langle\lambda_M\rangle)^d\}
\end{aligned}
\tag{4.10}
$$

and

$$
A_{kN} = \frac{1}{[(N-M)d-k]!}\lim_{s\to-\langle\lambda_N\rangle}\left(\frac{d}{ds}\right)^{(N-M)d-k}\{\Psi_d(s)(s+\langle\lambda_N\rangle)^{(N-M)d}\} \tag{4.11}
$$

Taking the inverse Laplace transform of $\Psi_d(s)$, the PDF is found to be

$$
\begin{aligned}
p_d(\gamma) &= L^{-1}\{\Psi_d(s)\} \\
&= \sum_{i=1}^{d}\left[A_{i1}\frac{\gamma^{i-1}}{(i-1)!}e^{-\gamma\langle\lambda_1\rangle} + A_{i2}\frac{\gamma^{i-1}}{(i-1)!}e^{-\gamma\langle\lambda_2\rangle} + \cdots + A_{iM}\frac{\gamma^{i-1}}{(i-1)!}e^{-\gamma\langle\lambda_M\rangle}\right] \\
&\quad + \sum_{k=1}^{(N-M)d} A_{kN}\frac{\gamma^{k-1}}{(k-1)!}e^{-\gamma\langle\lambda_N\rangle}
\end{aligned}
\tag{4.12}
$$

Hence, the CDF of the output SINR is :

$$
\begin{aligned}
P_d(\gamma) &= \int_0^{\gamma} p_d(\zeta)d\zeta \\
&= \sum_{i=1}^{d}\left\{\begin{aligned}&\frac{A_{i1}}{\langle\lambda_1\rangle^i}\left[1-\sum_{k=0}^{i-1}\frac{\gamma^k\langle\lambda_1\rangle^k}{k!}e^{-\gamma\langle\lambda_1\rangle}\right] + \frac{A_{i2}}{\langle\lambda_2\rangle^i}\left[1-\sum_{k=0}^{i-1}\frac{\gamma^k\langle\lambda_2\rangle^k}{k!}e^{-\gamma\langle\lambda_2\rangle}\right] \\ &+\cdots+\frac{A_{iM}}{\langle\lambda_M\rangle^i}\left[1-\sum_{k=0}^{i-1}\frac{\gamma^k\langle\lambda_M\rangle^k}{k!}e^{-\gamma\langle\lambda_M\rangle}\right]\end{aligned}\right\} \\
&\quad + \sum_{i=1}^{(N-M)d}\frac{A_{iN}}{\langle\lambda_N\rangle^i}\left[1-\sum_{k=0}^{i-1}\frac{\gamma^k\langle\lambda_N\rangle^k}{k!}e^{-\gamma\langle\lambda_N\rangle}\right]
\end{aligned}
\tag{4.13}
$$

C. BER PERFORMANCE FOR OPTIMUM COMBINING

By using an (*n,k*) convolutional encoder in the transmitter and the Viterbi soft decision decoder in the receiver, the first-event error probability for a path that differs from the correct (all-zero) path in *d* bits, can be computed as shown below. The unconditional first-event error probability $P_2(d)$ can then be computed by averaging the conditional first-event error probability $P_2(\gamma)$ over the PDF of output SINR, $p_d(\gamma)$. For BPSK signals, $P_2(\gamma) = Q(\sqrt{2\gamma})$ or $\frac{1}{2}\text{erfc}(\sqrt{\gamma})$, and the BER performance for optimum combining with multiple interferers using an adaptive array using a Viterbi decoder is determined using the PDF, $p_d(\gamma)$ derived in (4.12) as

$$P_2(d) = \int_0^\infty P_2(\gamma) p_d(\gamma) d\gamma$$

$$= \int_0^\infty \left\{ \sum_{i=1}^{d} \left[\begin{array}{l} A_{i1} \dfrac{\gamma^{i-1}}{(i-1)!} e^{-\gamma\langle\lambda_1\rangle} + A_{i2} \dfrac{\gamma^{i-1}}{(i-1)!} e^{-\gamma\langle\lambda_2\rangle} + \cdots \\ + A_{iM} \dfrac{\gamma^{i-1}}{(i-1)!} e^{-\gamma\langle\lambda_M\rangle} \end{array} \right] + \sum_{k=1}^{(N-M)d} A_{kN} \frac{\gamma^{k-1}}{(k-1)!} e^{-\gamma\langle\lambda_N\rangle} \right\} \frac{1}{2}\text{erfc}(\sqrt{\gamma}) d\gamma. \quad (4.14)$$

$$P_2(d) = \sum_{i=1}^{d} \left[\begin{array}{l} A_{i1}\mu_1^i \sum_{k=0}^{i-1} \binom{i+k-1}{k} \beta_1^k + A_{i2}\mu_2^i \sum_{k=0}^{i-1} \binom{i+k-1}{k} \beta_2^k + \cdots \\ + A_{iM}\mu_M^i \sum_{k=0}^{i-1} \binom{i+k-1}{k} \beta_M^k \end{array} \right] + \sum_{i=1}^{(N-M)d} A_{iN}\mu_N^i \sum_{k=0}^{i-1} \binom{i+k-1}{k} \beta_N^k \quad (4.15)$$

where

$$\mu_n = \frac{\sqrt{1+\langle \lambda_n \rangle}-1}{2\langle \lambda_n \rangle \sqrt{1+\langle \lambda_n \rangle}}$$

$$\beta_n = \frac{\sqrt{1+\langle \lambda_n \rangle}+1}{2\sqrt{1+\langle \lambda_n \rangle}}$$

The BER performance of BPSK versus the average branch SINR of adaptive antenna with several uncorrelated branches and several number of interferers is shown in Figure 4.2. Here, we use a ½ convolutional FEC with a constraint length of 8 and d_{free}=10 and $\beta_{10} = 2$, $\beta_{11} = 22$, $\beta_{12} = 60$, $\beta_{13} = 148$ and $\beta_{14} = 340$ [9]. Figure 4.3 shows the plot of BER performance of BPSK versus the total SNR of adaptive antenna without coding effect. The total input SNR, $N\Gamma_0$ is expressed as a function of average input SINR, Γ from (3.30). Figure 4.4 compares the BER performance with different total signal-to-interference ratio (SIR) and it is plotted by using the expression in (3.36) and under the same assumptions as made in Chapter III.

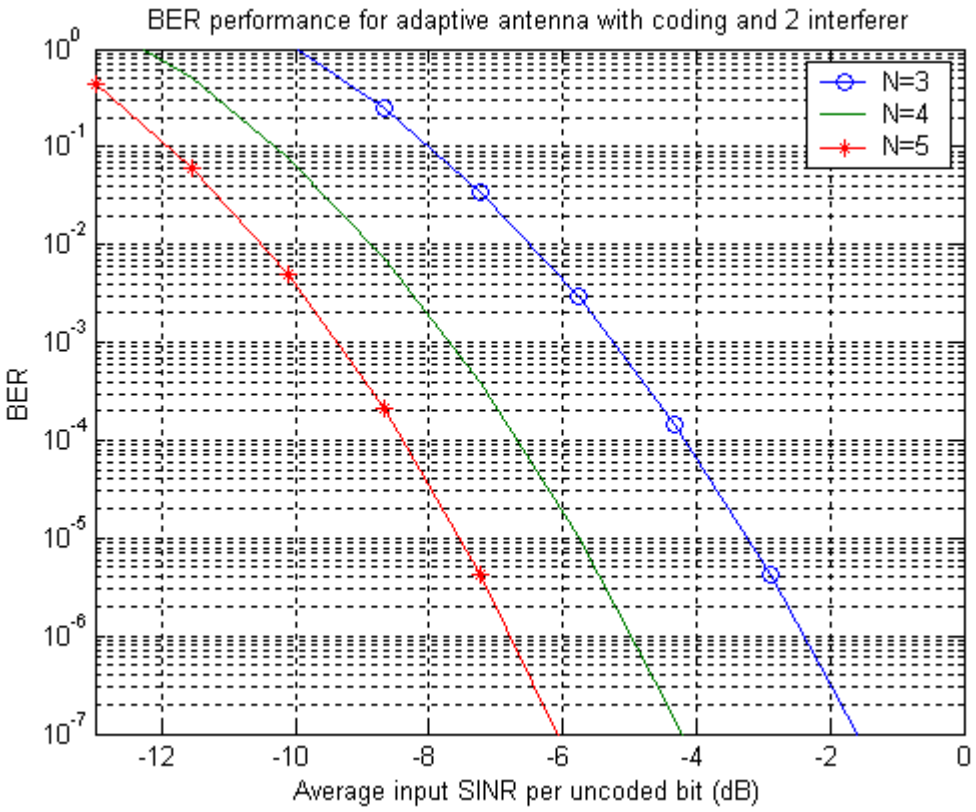

Figure 4.2. The BER performance of BPSK versus the average branch input SINR per uncoded bit for adaptive antenna with coding effect (*L=2,* $\Gamma_1 = \Gamma_2 = 3\,\mathrm{dB}$*)*.

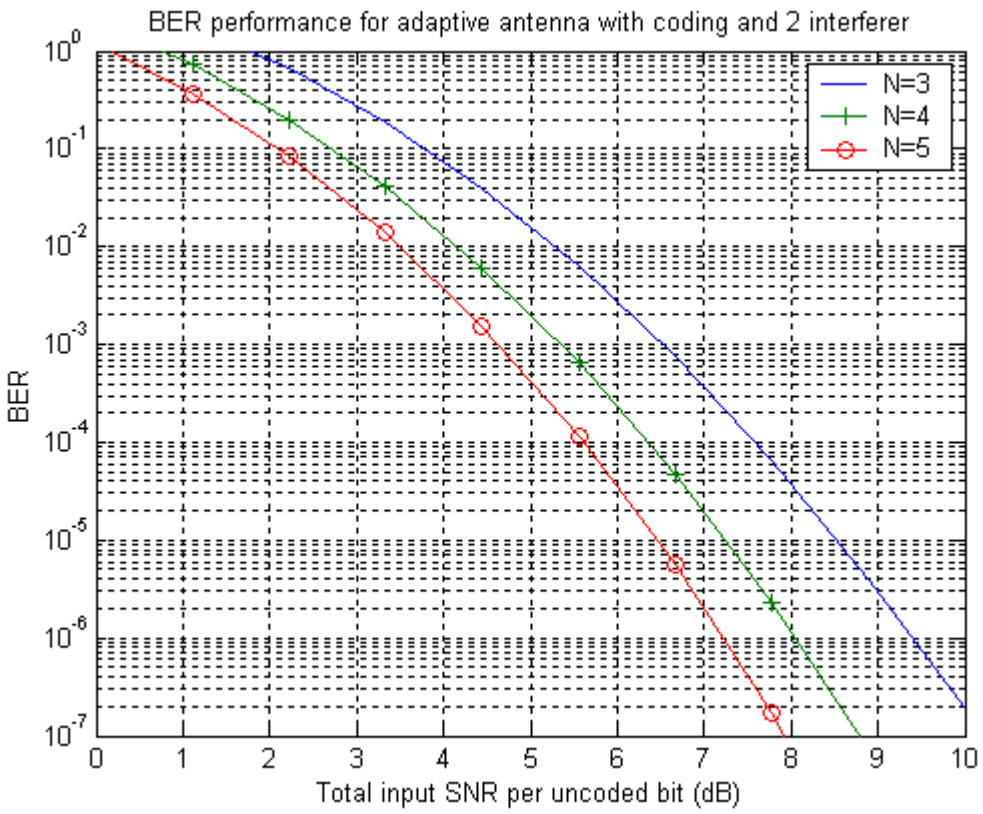

Figure 4.3. The BER performance of BPSK versus total SNR per unbcoded bit for adaptive antenna with coding effect (*L=2,* $\Gamma_1 = \Gamma_2 = 3\,\mathrm{dB}$*)*.

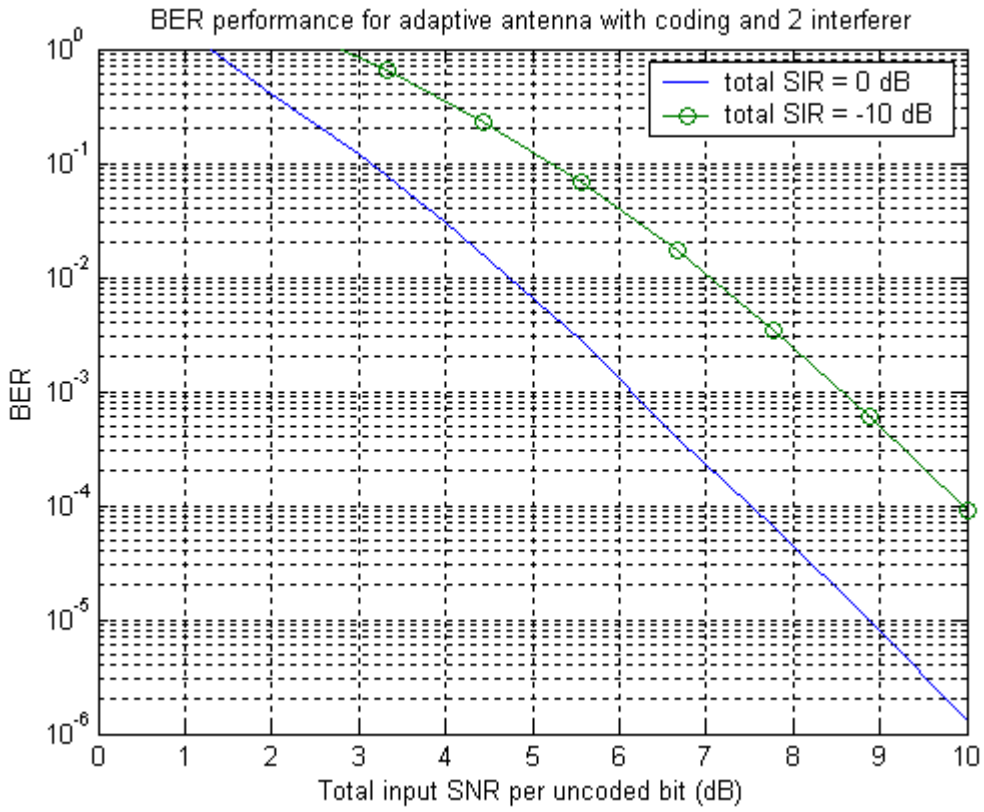

Figure 4.4. BER performance of BPSK versus the total SNR per uncoded bit of adaptive antenna with coding effect and different value of total SIR (*L=2,* $\Gamma_I = L\gamma_1 = 0\,\text{dB}$ or $-10\,\text{dB}$*)*.

In the absence of interference, the adaptive array works as a diversity antenna with maximum ratio combining (MRC) and with coding effect. In this case, the characteristic function in (4.8) becomes

$$\Psi_d(s) = \prod_{n=1}^{N}\left[\frac{\langle\lambda\rangle}{s+\langle\lambda\rangle}\right]^d = \left[\frac{\langle\lambda\rangle}{s+\langle\lambda\rangle}\right]^{dN} = \sum_{i=1}^{dN}\frac{A_i}{(s+\langle\lambda\rangle)^i} \tag{4.16}$$

where

$$A_i = \frac{1}{(dN-i)!}\lim_{s\to-\langle\lambda\rangle}\left(\frac{d}{ds}\right)^{dN-i}\{\Psi_d(s)(s+\langle\lambda\rangle)^{dN}\} \tag{4.17}$$

$$\langle \lambda \rangle = \frac{\sigma^2}{R_0} = \frac{\sigma^2}{P_0} = \frac{1}{\Gamma_0}$$

Again, the PDF can be found by taking the inverse Laplace transform of $\Psi_d(s)$,

$$\begin{aligned} p_d(\gamma) &= L^{-1}\{\Psi_d(s)\} \\ &= \sum_{i=1}^{dN} A_i \frac{\gamma^{i-1}}{(i-1)!} e^{-\gamma\langle\lambda\rangle} \end{aligned} \tag{4.18}$$

The BER performance of MRC with Rayleigh fading can be determined as follows:

$$\begin{aligned} P_2^{mrc}(d) &= \frac{1}{2}\int_0^\infty p_d(\gamma)\operatorname{erfc}(\sqrt{\gamma})d\gamma \\ &= \frac{1}{2}\int_0^\infty \left[\sum_{i=1}^{dN} A_i \frac{\gamma^{i-1}}{(i-1)!} e^{-\gamma\langle\lambda\rangle}\right]\operatorname{erfc}(\sqrt{\gamma})d\gamma \end{aligned} \tag{4.19}$$

Again, using the general integral formula in (3.33), we obtain

$$P_2^{mrc}(d) = \sum_{i=1}^{dN} A_i \left[\frac{\sqrt{1+\langle\lambda\rangle}-1}{2\langle\lambda\rangle\sqrt{1+\langle\lambda\rangle}}\right]^i \sum_{k=0}^{i-1}\binom{i+k-1}{k}\left[\frac{\sqrt{1+\langle\lambda\rangle}+1}{2\sqrt{1+\langle\lambda\rangle}}\right]^k \tag{4.20}$$

The upper bound on the first-event error probability, P_e, can be calculated as:

$$P_e \le \frac{1}{k}\sum_{d=d_{free}}^{\infty} \beta_d P_2^{mrc}(d) \tag{4.21}$$

The BER performance of BPSK versus the total SNR of adaptive antenna with several uncorrelated branches and several numbers of interferers is shown in Figure 4.5. Again, we use a ½ convolutional FEC with a constraint length of 8 and d_{free}=10. The BER plot in Figure 4.5 is seen to be consistent with the theory discussed in Proakis [8].

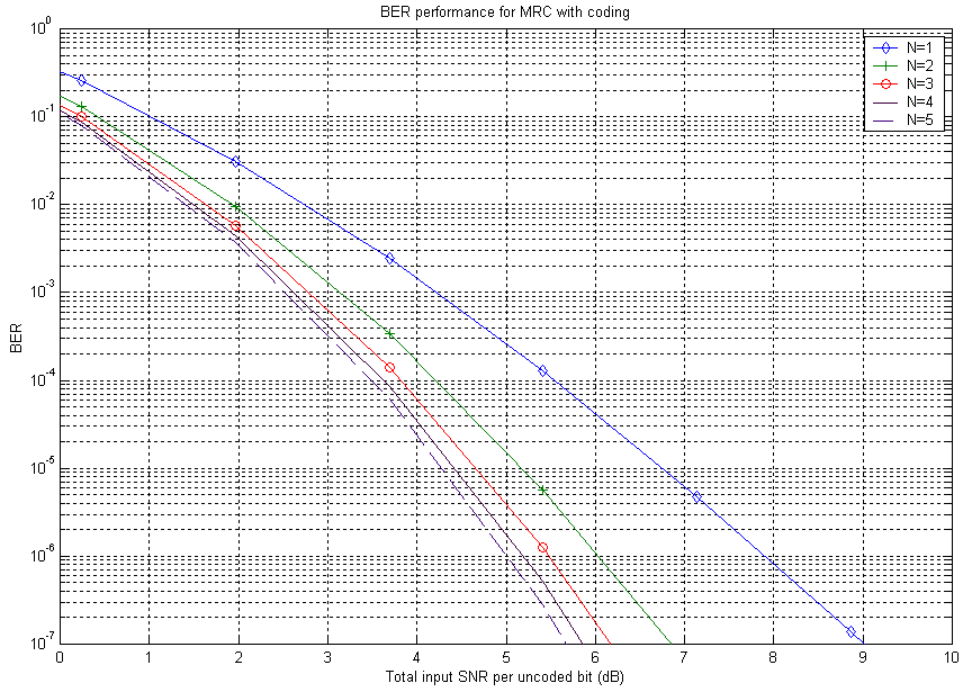

Figure 4.5. BER performance of BPSK versus the total SNR per uncoded bit, for adaptive antenna under Rayleigh fading with Maximal Ratio Combining (MRC) and coding.

THIS PAGE INTENTIONALLY LEFT BLANK

V. RAKE RECEIVER

As discussed in Chapter II, when uncorrelated multipath is present with the desired signal, the narrowband adaptive antenna array attempts to place nulls in the directions of all interferers. Thus the narrowband array results in a reduction in interference due to uncorrelated multipath, but it is a suboptimal solution because available path diversity is not being exploited. If the multipath components arrive in resolvable clusters, a spatial filtering Rake receiver can be used to resolve two uncorrelated components [10]. Figure 5.2 shows a spatial filtering Rake receiver.

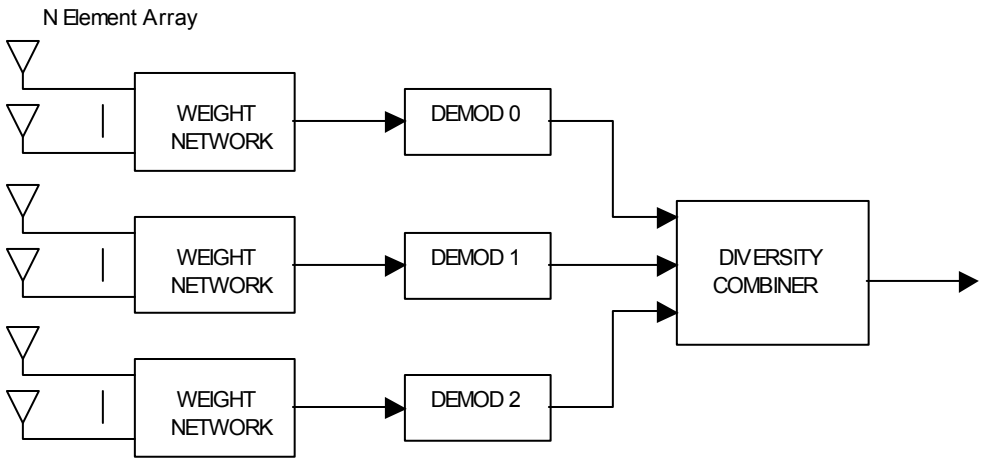

Figure 5.1. RAKE Receiver Model.

In this structure, each RAKE finger uses the adaptive antenna array to reject multipath components that are uncorrelated with the component to which the finger is locked. Diversity combining is then used to combine the output from each RAKE finger. Figure 5.2 illustrates the patterns used by each finger of the spatial filtering RAKE receiver. The spatial response for each finger of the receiver is adjusted to maximize the signal-to-interference-plus-noise (SINR) for that finger.

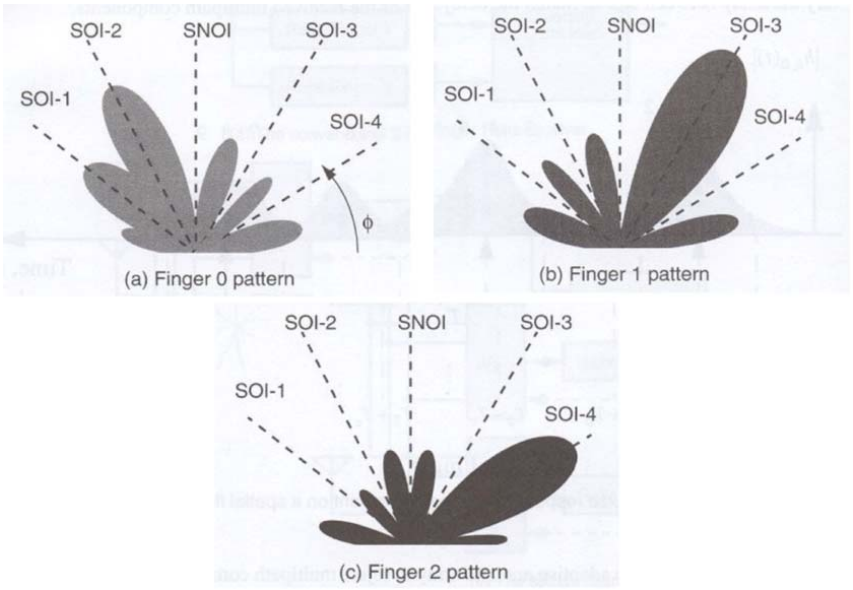

Figure 5.2. Antenna patterns obtained using a three finger spatial filtering Rake receiver receiving four components. The Signals –Of-Interest (SOIs) and Signals-Not-Of-Interest (SNOIs) are show as a function of Direction-Of-Arrival (From:10).

A. OUTPUT SIGNAL-TO-NOISE PLUS INTERFERENCE RATIO

From the discussion by Proakis [8], it is shown that a RAKE receiver processes the received signal in an optimum way to achieve the performance that is equivalent to an L_r^{th} -order diversity communication system. The optimum output SINR for RAKE receiver without coding effect can be derived as in [8], page 846, to be :

$$\gamma_{rake} = \sum_{k=1}^{L_r} \gamma_k \tag{5.1}$$

where L_r is the number of fingers at the RAKE receiver and γ_k is the output SINR at each finger of the RAKE receiver.

B. STATISTIC OF THE OUTPUT SINR

Using the same approach as in Chapter III and consistent with the discussion in Proakis [8], page 847, the characteristic function of γ_{rake} is

$$\begin{aligned}\Psi_{rake}(s) &= \left[\prod_{n=1}^{M}\left(\frac{\langle\lambda_n\rangle}{s+\langle\lambda_n\rangle}\right)^{L_r}\right]\left(\frac{\langle\lambda_N\rangle}{s+\langle\lambda_N\rangle}\right)^{(N-M)L_r} \\ &= \sum_{i=1}^{L_r}\frac{A_{i1}}{(s+\langle\lambda_1\rangle)^i}+\sum_{i=1}^{L_r}\frac{A_{i2}}{(s+\langle\lambda_2\rangle)^i}+\cdots+\sum_{i=1}^{L_r}\frac{A_{iM}}{(s+\langle\lambda_M\rangle)^i}+\sum_{k=1}^{(N-M)L_r}\frac{A_{kN}}{(s+\langle\lambda_N\rangle)^k} \\ &= \sum_{i=1}^{L_r}\left[\frac{A_{i1}}{(s+\langle\lambda_1\rangle)^i}+\frac{A_{i2}}{(s+\langle\lambda_2\rangle)^i}+\cdots+\frac{A_{iM}}{(s+\langle\lambda_M\rangle)^i}\right]+\sum_{k=1}^{(N-M)L_r}\frac{A_{kN}}{(s+\langle\lambda_N\rangle)^k}\end{aligned} \tag{5.2}$$

where

$$\begin{aligned}A_{i1} &= \frac{1}{(L_r-i)!}\lim_{s\to-\langle\lambda_1\rangle}\left(\frac{d}{ds}\right)^{L_r-i}\{\Psi_{rake}(s)(s+\langle\lambda_1\rangle)^{L_r}\} \\ A_{i2} &= \frac{1}{(L_r-i)!}\lim_{s\to-\langle\lambda_2\rangle}\left(\frac{d}{ds}\right)^{L_r-i}\{\Psi_{rake}(s)(s+\langle\lambda_2\rangle)^{L_r}\} \\ &\vdots \\ A_{iM} &= \frac{1}{(L_r-i)!}\lim_{s\to-\langle\lambda_M\rangle}\left(\frac{d}{ds}\right)^{L_r-i}\{\Psi_{rake}(s)(s+\langle\lambda_M\rangle)^{L_r}\}\end{aligned} \tag{5.3}$$

and

$$A_{kN} = \frac{1}{[(N-M)L_r-k]!}\lim_{s\to-\langle\lambda_N\rangle}\left(\frac{d}{ds}\right)^{(N-M)L_r-k}\{\Psi_{rake}(s)(s+\langle\lambda_N\rangle)^{(N-M)L_r}\} \tag{5.4}$$

Taking the inverse Laplace transform of $\Psi_{rake}(s)$, the PDF is found to be

$$\begin{aligned}p_{rake}(\gamma) &= L^{-1}\{\Psi_{rake}(s)\} \\ &= \sum_{i=1}^{L_r}\left[A_{i1}\frac{\gamma^{i-1}}{(i-1)!}e^{-\gamma\langle\lambda_1\rangle}+A_{i2}\frac{\gamma^{i-1}}{(i-1)!}e^{-\gamma\langle\lambda_2\rangle}+\cdots+A_{iM}\frac{\gamma^{i-1}}{(i-1)!}e^{-\gamma\langle\lambda_M\rangle}\right] \\ &\quad+\sum_{k=1}^{(N-M)L_r}A_{kN}\frac{\gamma^{k-1}}{(k-1)!}e^{-\gamma\langle\lambda_N\rangle}\end{aligned} \tag{5.5}$$

Here, again, we assume that there are M distinct eigenvalues, $M \leq N$, and one eigenvalue of multiplicity (N-M) in the most general case of interest.

C. BER PERFORMANCE FOR OPTIMUM COMBINING

Similarly, the expression for Probability of Bit Error can be derived to be

$$BER = \sum_{i=1}^{L_r} \left[\begin{array}{l} A_{i1}\mu_1^i \sum_{k=0}^{i-1} \binom{i+k-1}{k} \beta_1^k + A_{i2}\mu_2^i \sum_{k=0}^{i-1} \binom{i+k-1}{k} \beta_2^k + \cdots \\ + A_{iM}\mu_M^i \sum_{k=0}^{i-1} \binom{i+k-1}{k} \beta_M^k \end{array} \right] + \sum_{i=1}^{(N-M)L_r} A_{iN}\mu_N^i \sum_{k=0}^{i-1} \binom{i+k-1}{k} \beta_N^k \tag{5.6}$$

where

$$\mu_n = \frac{\sqrt{1+\langle \lambda_n \rangle} - 1}{2\langle \lambda_n \rangle \sqrt{1+\langle \lambda_n \rangle}}$$

$$\beta_n = \frac{\sqrt{1+\langle \lambda_n \rangle} + 1}{2\sqrt{1+\langle \lambda_n \rangle}}$$

The BER performance of BPSK versus the average branch SINR of adaptive antenna with RAKE receiver is shown in Figure 5.3 and the BER performance of BPSK versus total SNR of adaptive antenna with RAKE receiver is shown in Figure 5.4. Figure 5.5 shows the BER performance of BPSK versus total SNR of adaptive antenna with RAKE receiver and comparison between different total signal-to-interference ratios (SIR). In all the plots, we assume that there are 3 RAKE fingers (L_r = 3) which corresponds to 3 multipath components with signal strengths equal to that of the interference signals, hence a total of 4 undesired signals and 1 desired signal, since 2 interference signals are assumed here. With these assumptions, we have to use 5 antenna elements (N=5).

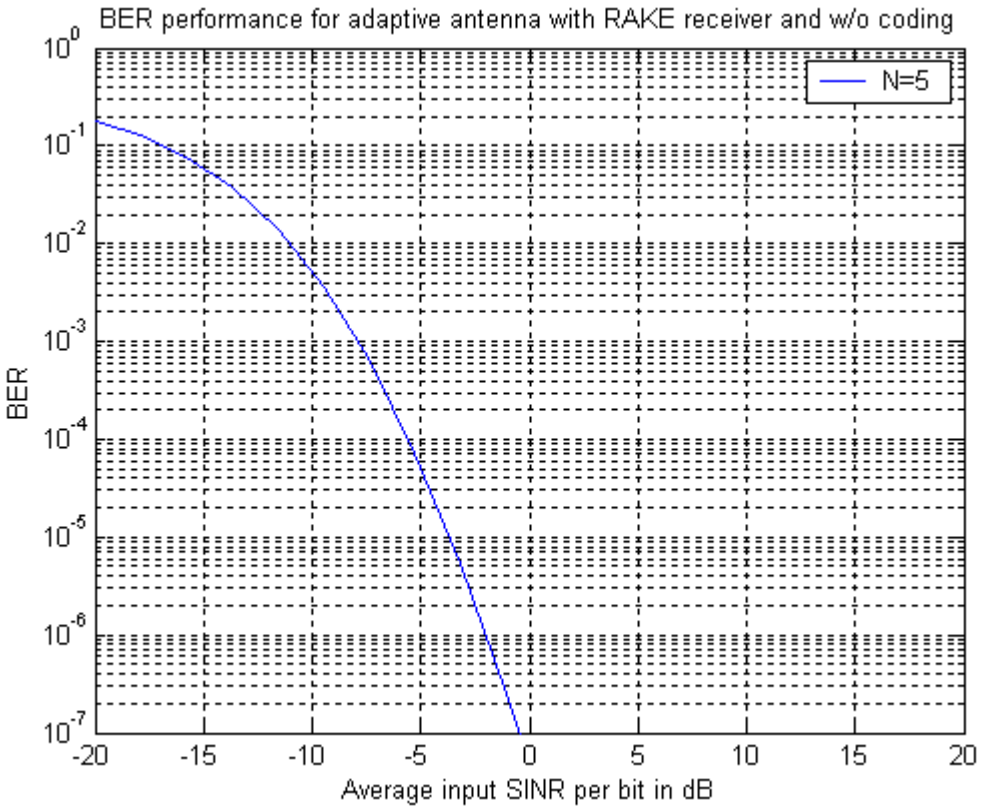

Figure 5.3. The BER performance of BPSK versus the average branch SINR per bit of adaptive antenna with RAKE receiver without coding (*L=4,* $\Gamma_1 = \Gamma_2 = \Gamma_3 = \Gamma_4 = 3\,\mathrm{dB}$*)*.

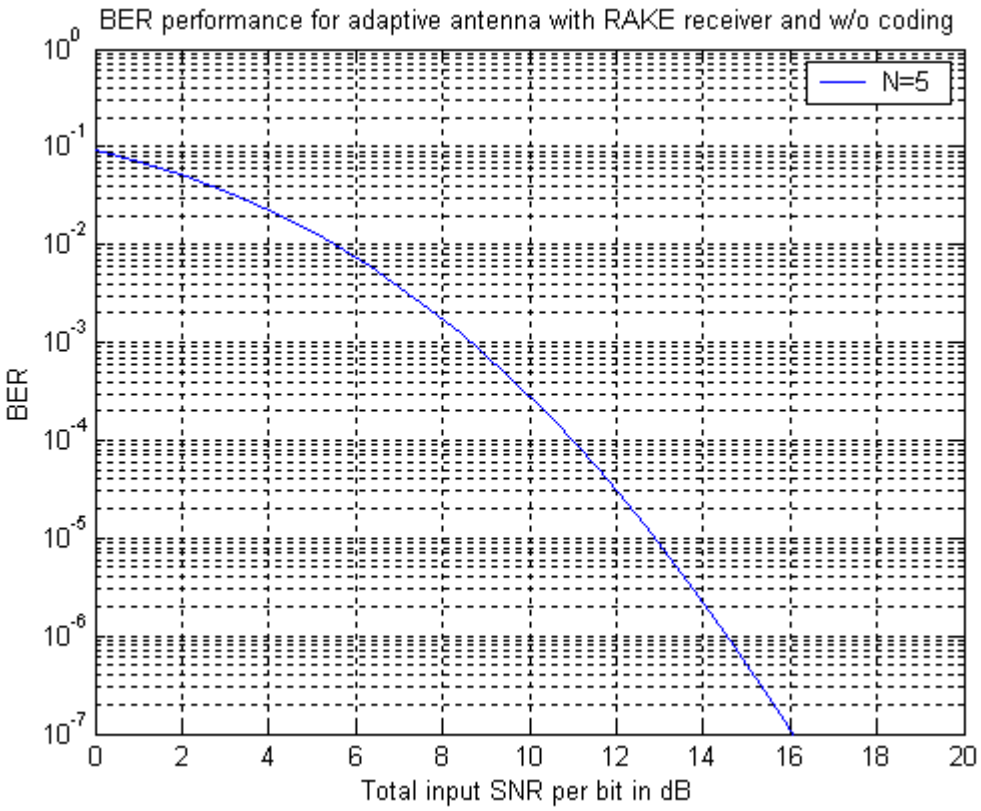

Figure 5.4. The BER performance of BPSK versus total SNR per bit of adaptive antenna with RAKE receiver without coding (*L=4,* $\Gamma_1 = \Gamma_2 = \Gamma_3 = \Gamma_4 = 3\,\mathrm{dB}$*)*.

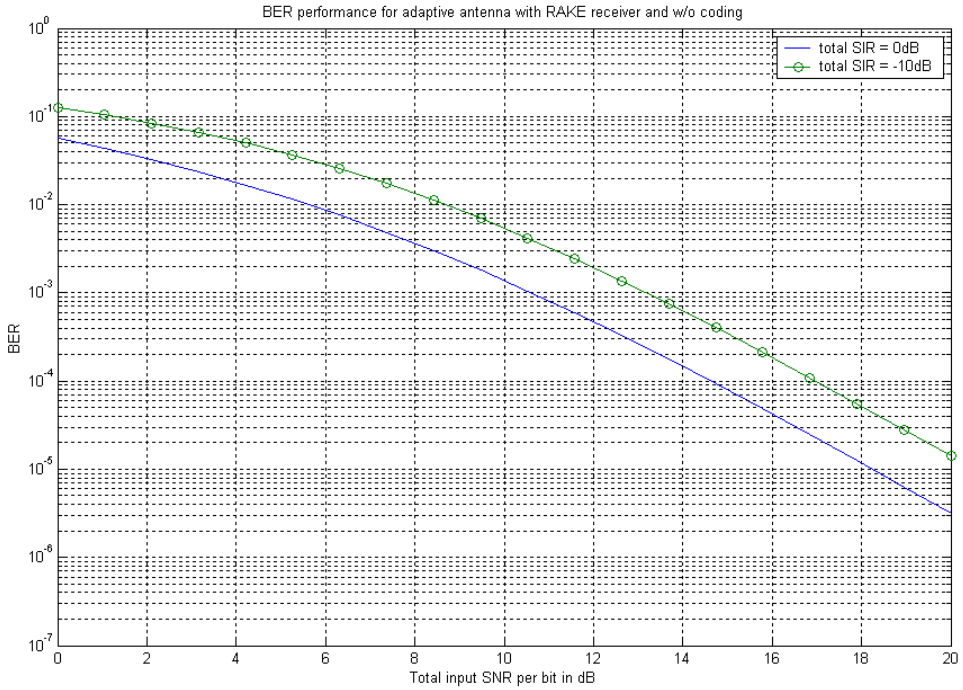

Figure 5.5. BER performance of BPSK versus the total SNR per bit of adaptive antenna with RAKE receiver without coding effect and different value of total SIR (*N*=5, *L=4,* $\Gamma_I = L\gamma_1 = 0$ dB or -10 dB*)*.

THIS PAGE INTENTIONALLY LEFT BLANK

VI. NUMERICAL RESULTS

In this chapter, using the equations derived in earlier chapters, we evaluate the performance of the adaptive antenna operating in a flat Rayleigh fading environment with coding and RAKE receiver and performance comparisons are made. Figure 6.1 shows the BER performance comparison of adaptive antenna working with coding and without coding. System performance with forward error correction (FEC) is evaluated using a ½ convolutional encoder with a constraint length of 8 as described in Chapter IV.

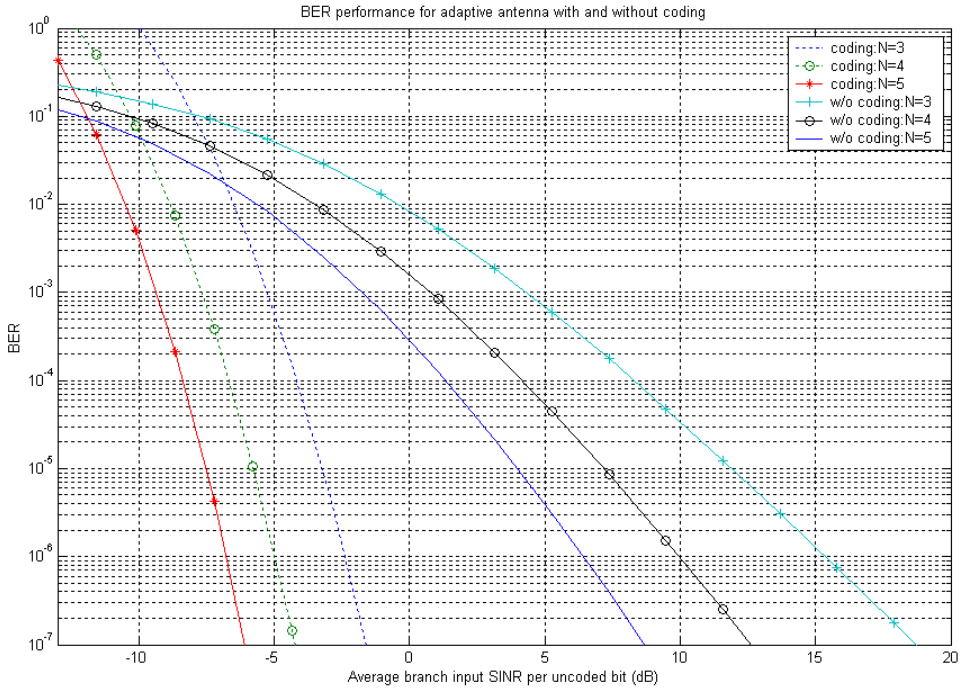

Figure 6.1. BER performance comparison for adaptive antenna with coding and without coding effect, plotting against average input SINR per uncoded bit

The upper bound for probability of error is calculated by evaluating equation (4.1) and (4.15), using the values of $P_2(d)$ for d=10 through 14, where d_{free}=10 and $\beta_{10} = 2$, $\beta_{11} = 22$, $\beta_{12} = 60$, $\beta_{13} = 148$ and $\beta_{14} = 340$ [9]. We assume 2 interferers (L=2) are present, with equal interference-to-noise ratios, $\Gamma_1 = \Gamma_2 = 3\,\text{dB}$. It can be seen from Figure 6.1 that by using FEC with adaptive antenna, the BER performance can be

improved by 17 dB or better as compared to the BER without using coding. The BER improves greatly by increasing the number of antenna elements.. Increasing the number of elements in the antenna array will increase the directivity and hence reduce the interference power and as a result improve the signal-to-interference-plus noise ratio (SINR). Figure 6.2 is the same as Figure 6.1 except that it is the plot of BER performance versus total SNR.

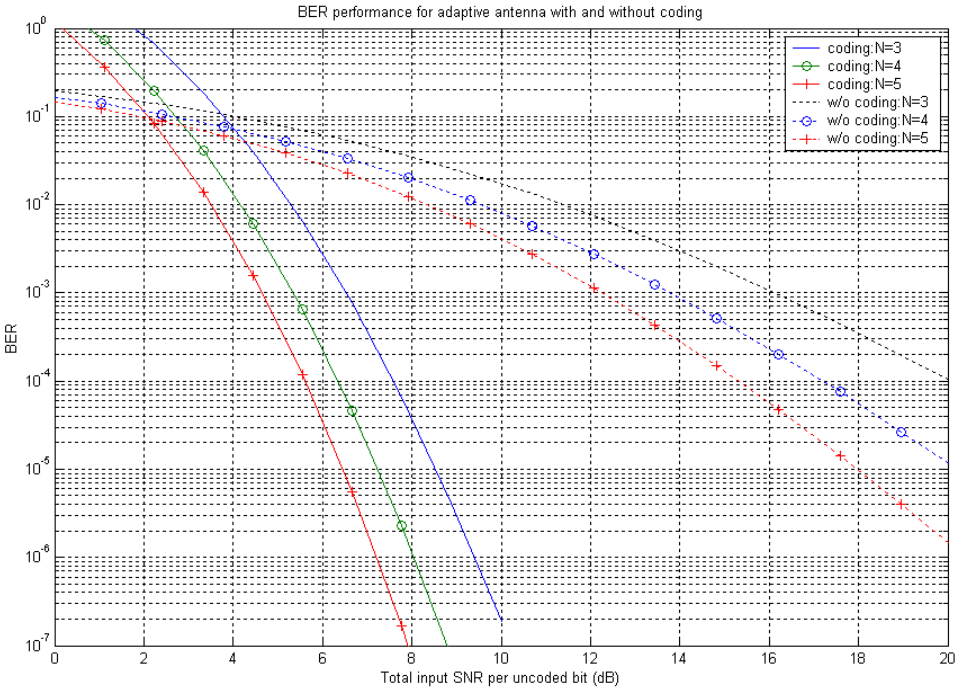

Figure 6.2. BER performance comparison for adaptive antenna with coding and without coding effect, plotting against total input SNR per uncoded bit.

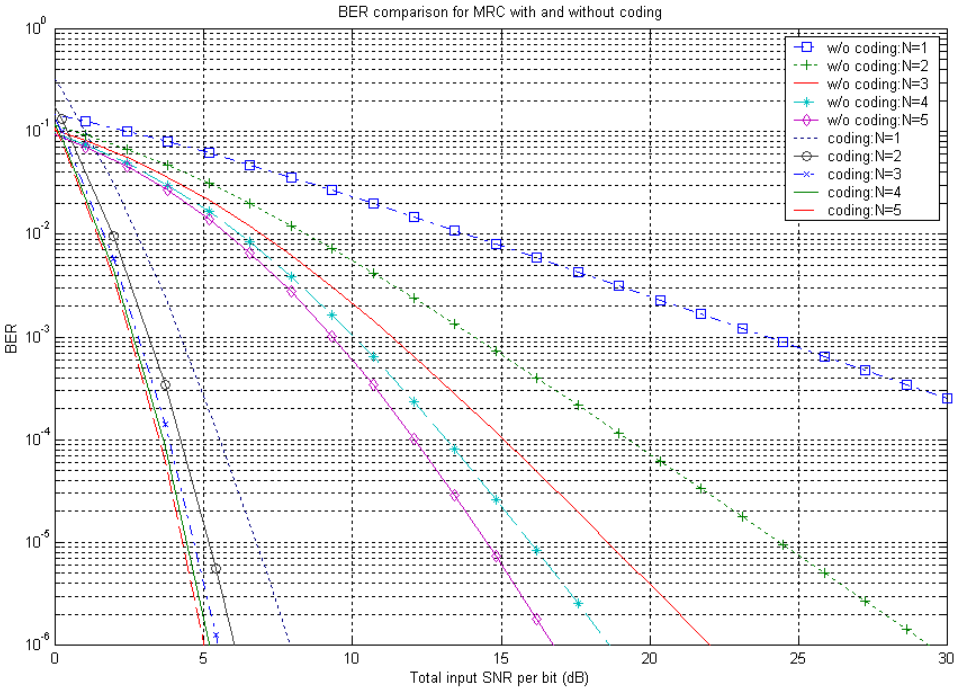

Figure 6.3. BER performance comparison for Maximal Ratio Combining (MRC) with coding and without coding effect per uncoded bit.

As discussed in Chapter III and IV, the adaptive antenna works like a Maximal Ratio Combiner (MRC) when there is no interference but only thermal noise. Figure 6.3 shows the BER comparison for MRC with and without coding. It can be seen that there is an improvement of at least 12 dB at BER of 10^{-6} when FEC is used. The effect of changing the number of antenna elements from 1 to 5 is also shown in Figure 6.3. The higher the number of antenna elements used, the greater is the diversity gain and hence better BER performance. Figure 6.4 compares the BER performance for an adaptive antenna with and without RAKE receiver and without coding effect. It can be seen that there is a 7 dB improvement for the adaptive antenna working with a RAKE receiver at BER of 10^{-7}.

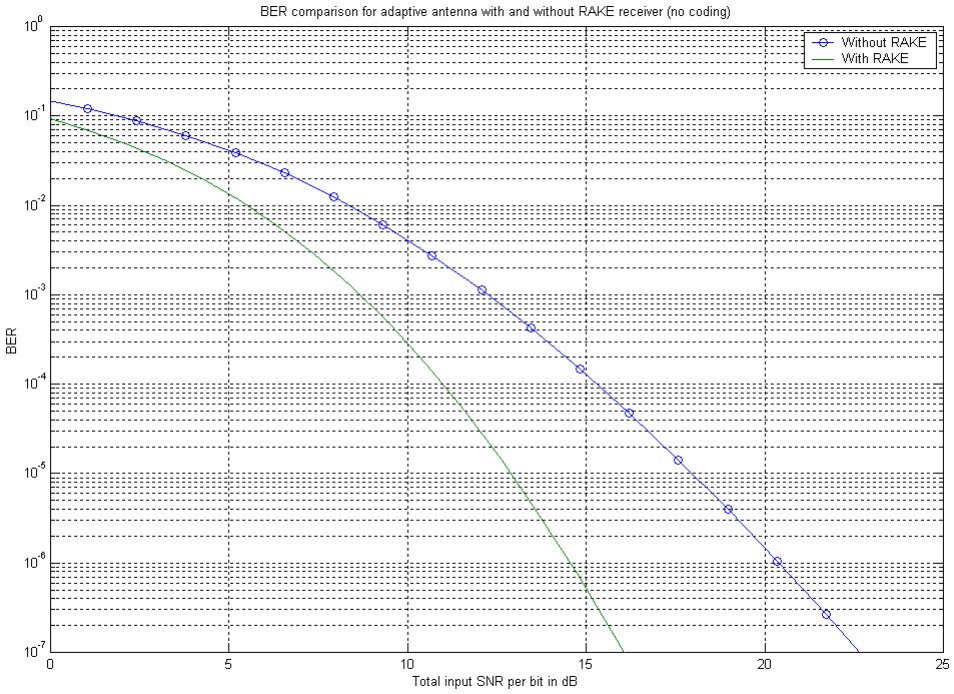

Figure 6.4. BER performance comparison for adaptive antenna with and without RAKE receiver with no coding effect (N=5, L=2 and L_r=3)

VII. CONCLUSIONS AND FUTURE WORK

A. CONCLUSIONS

In this thesis, an approximate analytical PDF andCDF for the output SINR of an adaptive antenna with uncorrelated branches and multiple interferers in flat Rayleigh fading environments has been derived. The intrinsic mean eigenvalues for systems with several branches and equal strength interferers have been presented and used to determine the mean eigenvalues for systems with arbitrary values of SINR and SNR. As a result closed-form expression for the BER for coherent PSK has been derived. With the analytic expressions for the CDF and the PDF available, the closed form expressions for the BER for all the other digital modulations can also be derived using the same approach discussed in the preceding chapters.

The effect of coding and RAKE receiver with adaptive antenna were also investigated and analyzed. By using forward error correction in the form of ½ rate convolutional coding with a constraint length of 8, the system performance in terms of bit error rates can be improved greatly due to the high coding gain achieved. To further improve the performance, a RAKE receiver can be used to combine the useful information in the multipath components and improve the signal-to-noise ratio.

The performance comparisons are made in terms of BER between adaptive antenna with coding effect and adaptive antenna without the effect of coding. The results shows that by using coding, there is at least a 13 dB improvement in SNR at BER of 10^{-4} and lower. By using a RAKE receiver with 3 fingers, which corresponds to 3 multipaths, the improvement in SNR at BER of 10^{-4} and lower is about 8 dB or better.

Without the presence of interference and with thermal noise as the only undesired signal, the adaptive antenna works like a Maximal Ratio Combiner (MRC). The performance of MRC with and without coding effect was also compared and the results show that there is a great improvement of at least 10 dB at BER of 10^{-4} and lower.

B. FUTURE WORK

As a future research subject, the performance analysis of adaptive antenna and the approach for developing the statistical output SINR and BER expressions for a narrowband signal can be extended to a wideband signal in a DS-CDMA cellular system operating in a Nakagami fading environment. The effect of correlated branches and unequal branch powers should also be investigated. In addition, other approaches such as using Moment Generating Function (MGF) can be explored to develop the statistic SINR and BER expressions for optimum combining using adaptive antennas.

LIST OF REFERENCES

1. J. H. Winters, "Optimum combining in digital mobile radio with cochannel interference," *IEEE Transactions on Vehicular Technology*, vol. VT-33, pp. 144-155, Aug 1984.

2. R. A. Monzingo and T. W. Miller, *Introduction to Adaptive Arrays,* New York: Wiley, 1980.

3. T. D. Pham and K. G. Balmain, "Multipath performance of adaptive antenna with multiple interferers and correlated fadings," *IEEE Transactions on Vehicular Technology*, vol. 48, no. 2, pp 342-352, Mar 1999.

4. R. Janaswamy, *Radiowave Propagation and Smart Antennas for Wireless Communications,* Boston, Massachusetts. Kluwer Academic Publishers, 2001.

5. U. Bhobe and P. L. Perini, "An Overview of Smart Antenna Technology for Wireless Communication," *IEEE Transactions on Communication,* pp 875-883, Oct 2000.

6. Papoulis, *Probability, Random Variables, and Stochastic Processes,* Boston, Massachusetts. WCB/McGraw-Hill, 1991.

7. P. Bello and B. D. Nelin, "Predetection diversity combining with selectively fading channels," *IRE Transaction on Communication System*, vol. CS-10, pp 32, Mar 1962.

8. J. G. Proakis, *Digital Communications, 4th Edition*, New York/McGraw-Hill, 2001.

9. J. E. Tighe, "Modeling and Analysis of Cellular CDMA Forward Channel," Dissertation, Naval Postgraduate School, Monterey, CA, March 2001.

10. C. Liberti, Jr and S. Rappaport, *Smart Antennas for Wireless Communications*, Prentice Hall, 1999.

THIS PAGE INTENTIONALLY LEFT BLANK

INITIAL DISTRIBUTION LIST

1. Defense Technical Information Center
   Ft. Belvoir, VA

2. Dudley Knox Library
   Naval Postgraduate School
   Monterey, CA

3. Chairman
   Department of Electrical and Computer Engineering
   Naval Postgraduate School
   Monterey, CA

4. Professor Tri T. Ha
   Department of Electrical and Computer Engineering
   Naval Postgraduate School
   Monterey, CA

5. Professor David Jenn
   Department of Electrical and Computer Engineering
   Naval Postgraduate School
   Monterey,CA

6. Professor Jovan Lebaric
   Department of Electrical and Computer Engineering
   Naval Postgraduate School
   Monterey,CA

7. Kaiser Tan Beng Kiat
   Blk 367 Woodlands Ave 5, #07-452. Singapore 730367